Performance Analysis of Rayleigh Fading and Cochannel Interference in Wireless Communication

Chunjun Gao, Alexander M. Haimovich

Final Technical Report

Center for Communications and Signal Processing Research
University Heights, Newark, NJ 07102

NJIT
New Jersey Institute of Technology

REPORT DOCUMENTATION PAGE

Form Approved
OMB No. 0704-0188

PLEASE DO NOT RETURN YOUR FORM TO THE ABOVE ADDRESS.

1. REPORT DATE *(DD-MM-YYYY)*	2. REPORT TYPE	3. DATES COVERED *(From - To)*
1 April 2000	Final Technical Report	April 1997 - December 1999

4. TITLE AND SUBTITLE

Adaptive Space-Time, Processing for High Performance, Robust Military Wireless Communications

5a. CONTRACT NUMBER

5b. GRANT NUMBER

F49620-97-1-0241

5c. PROGRAM ELEMENT NUMBER

6. AUTHOR(S)

Alexander M. Haimovich

5d. PROJECT NUMBER

5e. TASK NUMBER

5f. WORK UNIT NUMBER

7. PERFORMING ORGANIZATION NAME(S) AND ADDRESS(ES)

Air Force Office of Scientific

8. PERFORMING ORGANIZATION REPORT NUMBER

9. SPONSORING/MONITORING AGENCY NAME(S) AND ADDRESS(ES)

Dr. Jon A. Sjogren
Air Force Office of Scientific Research
801 N. Randolph Street
Arlington, VA 22203-1977

10. SPONSOR/MONITOR'S ACRONYM(S)

11. SPONSOR/MONITOR'S REPORT NUMBER(S)

12. DISTRIBUTION/AVAILABILITY STATEMENT

Distribution Unlimited

13. SUPPLEMENTARY NOTES

14. ABSTRACT

This report summarizes work on several topics related with the application of space-time processing to wireless communications: (1) performance of adaptive arrays for wireless communications over fading channels in the presence of cochannel interference, particulalry the case when the number of interference sources exceeds the array degrees of freedom, (2) derivation of exact bit error probability for the detection of coherent binary PSK signals of the optimum combiner employing space diversity when both the desired signal and a Gaussian co-channel interferer are subject to flat Rayleigh fading, (3) the application of adaptive arrays to relax power control requirements in CDMA communications, (4) the application of reduced-rank methods for improving wireless communication links in the presence of unknown interference. The work provides a better understanding and contributes new algorithms for the application of space-time to wireless communications.

15. SUBJECT TERMS

Fading channel, space diversity, smart antennas, adpative arrays.

16. SECURITY CLASSIFICATION OF:			17. LIMITATION OF ABSTRACT	18. NUMBER OF PAGES	19a. NAME OF RESPONSIBLE PERSON
a. REPORT	b. ABSTRACT	c. THIS PAGE			Alexander M. Haimovich
NC	NC	NC		73	19b. TELEPHONE NUMBER *(Include area code)* 973-596-3534

April 2000 Final Report Grant F49620-97-1-0241, Apr. 97 - Dec. 99

Adaptive Space-Time Processing for High Performance, Robust Military Wireless Communications

Alexander M. Haimovich

New Jersey Institute of Technology, Newark, NJ

Air Force Office of Scientific Research
801 N. Randolph St.
Arlington, Va. 22203-1977

Adaptive antenna arrays and space-time processing are important resources for military wireless communications. This report summarizes work on several topics related with the application of space-time processing to wireless communications: (1) performance of adaptive arrays for wireless communications over fading channels in the presence of cochannel interference (CCI), particulalry the case when the number of interference sources exceeds the array degrees of freedom, (2) derivation of exact bit error probability (BEP) for the detection of coherent binary PSK signals of the optimum combiner employing space diversity when both the desired signal and a Gaussian co-channel interferer are subject to flat Rayleigh fading, (3) the application of adaptive arrays to relax power control requirements in CDMA communications, (4) the application of reduced-rank methods for improving wireless communication links in the presence of unknown interference. Results are demonstrated by analysis and illustrated by numerical simulations. The work provides a better understanding and contributes new algorithms for the application of space-time to wireless communications.

73

UNCLASSIFIED UNCLASSIFIED UNCLASSIFIED UL

Contents

List of Figures

Chapter 1

Executive Summary

This document presents the final technical report on work done between April 1997 to December 1999 on "Adaptive Space-Time Processing for High Performance, Robust Military Wireless Communications". The work studied the operation of adaptive arrays in fading channels and developed algorithms for fading mitigation and interference cancellation. The research spread over several topics. These topics and associated main results are summarized below.

We studied the performance of adaptive arrays for wireless communications over fading channels in the presence of cochannel interference (CCI). In particular, we studied the case when the number of interference sources exceeds the number of degrees of freedom. Such case is of interest in wireless communications when practical considerations dictate a small number of antennas in the array and there are multiple interference sources competing with the signal of interest. We analyzed the performance of adaptive arrays in Rayleigh and Ricean channels. The main contribution of this analysis is the development of the theory when both the signal of interest (SOI) and the cochannel interference (CCI) are assumed subject to fading conditions. We considered BPSK signalling in flat, quasi-static channels. Rayleigh or Rice fading was assumed for the SOI, while CCI was assumed subject to Rayleigh fading. Using a multivariate statistical analysis approach and assuming equal-power interference sources, analytical expressions were derived for the density function of the array output signal-to-interference ratio (SIR), the outage probability, and the average probability of bit error with two methods of antenna combining: maximal ratio combining and optimum combining [1, 2]. A limited analysis of the equal gain combiner was also obtained.

When the number of interference sources is smaller than the number of degrees of freedom, and if optimum combining is applied, the interference is canceled by the array. We derived expressions for the *exact* bit error probability (BEP) for the detection of coherent binary PSK signals of the optimum combiner employing space diversity when *both* the desired signal and a Gaussian co-channel interferer are subject to flat Rayleigh fading [3]. Two different methods were employed to reach two different, but numerically identical, expressions. With the *direct* method the conditional BEP is averaged over the fading of both signal and interference.

We studied various aspects of the application of space-time processing to CDMA communications. In particular, we studied the relation between power control error and array processing for spatial diversity. It is well known that the capacity of CDMA systems degrades rapidly with the increase in power control error. The performance of CDMA systems

is also affected by factors such as large-scale fading, small-scale fading, and CCI. Most of the published research on the performance analysis of CDMA systems usually accounts for subsets of these factors. We provided a comprehensive analysis which takes into account the joined effect of several of the most important factors affecting the performance of CDMA systems. In particular, we developed new analytical expressions for the outage and bit error probability of CDMA systems. These expressions account for adverse effects such as path loss, large-scale fading (shadowing), small-scale fading (Rayleigh fading), and CCI, as well as for correcting mechanisms such as power control error (compensates for path loss and shadowing), spatial diversity (mitigates against Rayleigh fading), and voice activity gating (reduces CCI). This work is disseminated in [4, 5, 6, 7].

Space-time adaptive processing (STAP) can be applied to improve performance of both CDMA and TDMA communications systems. In previous work we have shown that STAP applied to CDMA systems is an efficient means to increase capacity by providing diversity paths to combat multipath and by suppressing interferences through spatial-temporal filtering. We studied the application of the eigencanceler, a reduced rank method based on the eigendecomposition of the estimated covariance matrix, to the wireless communication problem. Simple closed-form bounds were obtained for the bit error rate of BPSK modulation in the presence of cochannel interference in systems using sample matrix inversion (SMI) and the eigencanceler. The application of SMI and the eigencanceler to a flat fading TDMA system was studied in the context of the IS-54/IS-136 standard. It was shown that adaptive antennas in conjunction with reduced-rank processing can be used to increase capacity of such systems by reducing the frequency reuse factor from 7 to 1 [8, 9, 10].

Chapter 2

Introduction

In wireless communications, the presence of cochannel interference (regardless of cell size) limits the system capacity, whereas multipath fading limits the system performance. Hence, methods that address these problems are of great interest. Antenna arrays, with different combining methods, have been shown to combat both multipath fading of the desired signal and cochannel interference (CCI), subsequently increasing the performance of mobile radio systems. The combining methods, which mainly include Equal Gain Combining (EGC), Maximal Ratio Combining (MRC) and Optimum Combining (OC), can make antenna arrays provide diversity paths to combat multipath fading of the desired signal and reduce the power of interfering signals at the receiver.

With EGC all antenna channels are provided with equal gain, but varying phase to match the phase shift in the multipath fading channel. With MRC and OC, both gain and phase are controlled. MRC is the optimum linear combining technique for coherent reception with independent fading at each antenna element in the presence of spatially white Gaussian noise [11]. The complex weight at each element compensates for the phase shift in the channel and is proportional to the signal strength. MRC mitigates fading, however, it ignores cochannel interference (CCI). OC addresses both problems of multipath fading of the desired signal and the presence of CCI. With OC, the signals received by several antenna elements are weighted and combined to maximize the output signal-to-interference-plus-noise ratio (SINR) [12].

A growing body of work is available on antenna arrays in wireless. Works that consider diversity reception in Rayleigh/Ricean/Nakagami channels, but no cochannel interference (CCI), include [13, 14, 15, 16, 17]. The case of a single CCI was analyzed in [12, 18, 19]. The effect of CCI and fading was studied in [20], but that work did not consider diversity or combining methods. The performance of adaptive arrays with Optimum Combining (OC) in Rayleigh fading and equal-power CCI sources is reported in [1], and with arbitrary power interferers in [21].

Chapter 2 contains the signal models used in this report. In Chapter 3, we expand on previous work by studying the performance of wireless systems with adaptive arrays utilizing Equal Gain Combining (EGC) and Maximal Ratio Combining (MRC) in Rayleigh/Rice fading in the presence of multiple equal-power CCI sources. We also expands [1] by considering Optimum Combining in the Ricean channel case. The emphasis is on obtaining closed-form expressions.

In [22, 23], a closed form expression is given for the bit error rate (BEP) of the optimum combiner of BPSK signals with flat Rayleigh fading and a co-channel interferer (CCI). The optimum combiner, in the context of this paper, refers to an antenna array that maximizes the signal-to-interference-plus-noise ratio (SINR) at the array output. The expression in [2, eq. (25)], was derived without explicitly taking into account the fading of the CCI. Rather, the CCI power *averaged* over fading was used in the derivation.

We provide an *exact* result with Optimum Combining in Chapter 4 , in which the BEP is first expressed *conditional* on the fading of both signal of interest (SOI) and CCI. The average BEP is subsequently derived by taking the expectation with respect to the fading of both SOI and CCI.

Due to the complexity of CDMA communications scenario, most published results account for only some of the adverse effects of large-scale fading, small-scale fading , power control error (PCE) and cochannel interference etc. For example, the performance analysis related to the log-normal interference can be found in [24, 25, 26, 27, 28, 29], however the cited work does not consider small-scale fading effects. The performance analysis with both fading and shadowing is considered in several recent publications [30, 31, 32, 33, 34, 35]. However, results are published either as simulations or as approximations, which generally lack accuracy at low PCE. For accurate predictions of CDMA systems performance, it is of great interest to be able to develop closed-form expressions that simultaneously incorporate the effects of shadowing, power control error, Rayleigh fading, voice activity and space-time processing.

The work in Chapter 5 attempts to provide more complete answers to the reverse link performance of wireless CDMA with Maximal Ratio Combining , and to develop expressions for the outage probability and probability of bit error, while taking into account multiple effects.

We investigate the application of a reduced-rank method referred to as *eigencanceler* to implement an optimum combiner in a flat fading Rayleigh channel with unknown cochannel interference. It is well known in array processing that a loss in the signal-to-noise and interference ratio (SNIR) occurs when the array covariance matrix is estimated from a limited size training set. In work motivated by radar applications, it was found that reduced-rank methods can significantly reduce these losses by providing improved statistical stability [36, 37].

In Chapter 6, we are concerned with the effects of training data on the performance of adaptive arrays for wireless communications in the following cases: (1) an optimum combiner of BPSK signals in a flat Rayleigh fading channel in the presence of cochannel interference (CCI), and (2) a system modeled after the IS-54/IS-136 standard utilizing optimum combining with multiple CCI sources.

Chapter 3

Signal Model

In this chapter, the mathematical model for the type of signals addressed in the report is presented. Since part of the report deals with CDMA signals, the signal model for CDMA is also introduced. The following notation is adopted: boldface lower case letters denote vectors, boldface upper case letters denote matrices, the superscript H denotes Hermitian transpose.

Consider the uplink of a mobile communication system employing a base station with an N element linear antenna array. The number of antenna elements is N and the number of cochannel interferers is L. After coherent demodulation and matched filtering, the array output sampled at $t = kT$ is represented by the N dimensional vector

$$\mathbf{u}[k] = \sqrt{P_s}\mathbf{c}_s z_s[k] + \sum_{i=1}^{L} \sqrt{P_i} z_i[k]\,\mathbf{c}_i + \mathbf{n}[k], \tag{3.1}$$

where $\sqrt{P_s}$, $\sqrt{P_i}$ are respectively, the signal and CCI amplitudes, the data symbols $z_s[k]$ are mutually independent and assume values $\in \{-1, 1\}$ with equal probabilities, and $\mathbf{n}[k]$ is the vector of ambient noise. The noise is complex-valued, stationary, zero-mean white Gaussian with covariance matrix $E\left[\mathbf{n}\mathbf{n}^H\right] = N_o\mathbf{I}$. The quantity $z_i[k]$ incorporates information on the ith CCI and is given by [20]

$$z_i[k] = \sum_{m=-\infty}^{\infty} b_i[m]\, g(kT - mT - \tau_i) \tag{3.2}$$

where the CCI symbols $b_i[m]$ assume values $\in \{-1, 1\}$ with equal probability, are mutually independent, and are independent of $z_s[k]$. The equivalent impulse response of the transmitter, channel and receiver $g(t)$ has a raised cosine pulse shape with excess bandwidth β. The random variable τ_i represents the timing phase of the ith CCI and is assumed uniformly distributed over the interval $[0, T]$, where T is the symbol interval. CCI samples $z_i = z_i[k]$, have the following properties: (1) $E[z_i] = 0$ (since $E[b_i[k]] = 0$), (2) due to the independence between interference sources, the random variables z_i are mutually independent (hence, $E[z_i z_j] = 0$ for $i \neq j$), and (3) $E[z_i^2] = 1 - \beta/4$ (see [20]). It is assumed that transmission of the signal takes place in a flat fading Rayleigh channel in the presence of additive white Gaussian noise and CCI.

The vectors $\mathbf{c}_s$ and $\mathbf{c}_i$ respectively, represent the channel complex gains for the signal and CCI. Sometimes, we express $\mathbf{c}_s$ and $\mathbf{c}_i$ as $\mathbf{c}_s^T = \left[\alpha_{s,1}, \alpha_{s,1}e^{j\phi_{s,2}} \ldots, \alpha_{s,N}e^{j\phi_{s,N}}\right]$, $\mathbf{c}_i^T = \left[\alpha_{i,1}, \alpha_{i,1}e^{j\phi_{i,2}} \ldots, \alpha_{i,N}e^{j\phi_{i,N}}\right]$, where α_s is the channel amplitude gain, ϕ_s is the total transmitter-to-receiver carrier phase shift due to their spatial separation and the random phase introduced by the fading channel, the random phases ϕ_i of the interfering carriers are assumed uniformly distributed over the interval $[0, 2\pi]$, and α_i are random variables representing the gain of the fading channel for the ith interferer. The channel vectors are mutually independent, but have identical distributions, which are complex-valued, zero-mean, multivariate Gaussian with independent terms and σ_s^2 variance, i.e., for example $E\left[\mathbf{c}_s\mathbf{c}_s^H\right] = \sigma_s^2\mathbf{I}$.. The fading is assumed quasi-static, i.e., channel vectors are fixed over some time interval of interest referred to as frame, but vary independently from frame to frame.

It is further assumed that the interference-plus-noise vector

$$\mathbf{x}[k] = \sum_{i=1}^{L} \sqrt{P_i} z_i[k]\, \mathbf{c}_i + \mathbf{n}[k] \tag{3.3}$$

has a multivariate Gaussian distribution with zero-mean and covariance

$$E\left[\mathbf{x}[k]\,\mathbf{x}[k]^H\right] = \mathbf{R}$$

where

$$\mathbf{R} = \sum_{i=1}^{L} P_i \mathbf{c}_i \mathbf{c}_i^H + \sigma\mathbf{I} \tag{3.4}$$

is the (colored) noise covariance matrix.

Signal Model for CDMA

This system model represents the reverse link of a single cell CDMA system which serves K_u users, and uses a base station with an M-element antenna array. The received signals are assumed to undergo independent, flat Rayleigh fading. It is further assumed that the fading is slowly varying such that the lowpass equivalent channel seen by each antenna can be characterized by a complex-valued scalar. The system is assumed interference limited with negligible thermal noise. The CDMA reverse link receiver model is shown in Figure 3.1.

The complex envelope of the signal received at the base station is then expressed by the M-dimensional vector:

$$\mathbf{x}(t) = \sqrt{\lambda_1}\, m_1(t-\tau_1)u_1(t-\tau_1)\mathbf{c}_1 + \sum_{k=2}^{K_u} \epsilon_k \sqrt{\lambda_k}\, m_k(t-\tau_k)u_k(t-\tau_k)\mathbf{c}_k, \tag{3.5}$$

where the first and second terms respectively, represent the desired signal and the CCI, λ_k $(k = 1, \cdots, K_u)$ are the powers of the received signals, $\mathbf{c}_k$ are normalized complex Gaussian

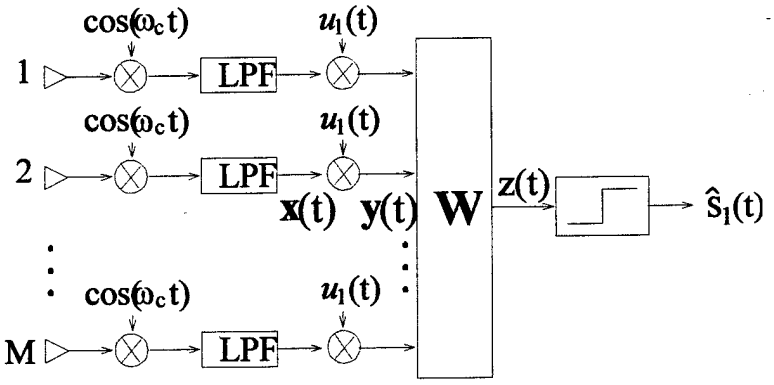

Figure 3.1: CDMA reverse link receiver model

channel vectors with $E\left[\mathbf{c}_k\mathbf{c}_k^H\right] = \mathbf{I}$, $\mathbf{I}$ is the $M \times M$ identity matrix, $m_k(t)$ are NRZ waveforms of the users' data, $u_k(t)$ are the spreading sequences, ϵ_k are binary random variables indicating the users' voice activity, τ_k are the users' delays. Let $m_k(t) = \sum_i s_k(i)\, h(t - iT_s)$, where $h(t)$ is the basic pulse shape, T_s is the symbol interval, i is the symbol interval index, and $s_k(i) \in \{-1, 1\}$ are the users' binary data. It is assumed that $E[s_k(i)] = 0$, and $E[s_k(i)\, s_l(j)] = \delta_{kl}\delta_{ij}$, where $\delta_{ij} = 1$ for $i = j$, and $\delta_{ij} = 0$ otherwise. The signature waveforms are normalized to unit energy over the symbol interval. For convenience, $\tau_1 = 0$. In a system that provides a single service (such as voice) with the same bit error rate and with perfect power control, all λ_k's are equal. The received powers λ_k, $k = 1, \ldots, K_u$, are the result of path loss, shadowing and imperfect power control, and are modeled as independent, identically distributed (i.i.d.) random variables with log-normal distribution. If λ_k has a log-normal distribution, then the received power expressed in dB, $\alpha_k = 10\log_{10}\lambda_k$ has a normal distribution with mean m_α and variance σ_α^2. The standard deviation of α_k is the PCE measured in dB. Since $\alpha_k < m_\alpha$ with probability $\frac{1}{2}$, $10^{m_\alpha/10}$ is the median value of λ_k. The voice activity ϵ_k is modeled as a Bernoulli (p) random variable with Pr $(\epsilon_k = 1) = p$, where p is the *voice activity factor*.

Chapter 4

Combining Methods

In this chapter, we are concerned with the flat (nondispersive), quasi-static fading channel, in which a desired signal competes with multiple CCI sources. The performance of adaptive arrays is studied for several channel models of the signal of interest (SOI): Rayleigh, Rice, non-fading. In all cases, the interference is assumed subject to Rayleigh fading. Channels associated with interference sources are assumed independent and identically distributed. It is further assumed that the fading is slow and that the receiver has perfect knowledge of the instantaneous channel realization and a coherent receiver can be implemented. The system is assumed interference limited. It is also assumed that the degrees of freedom are insufficient to remove all interferers, hence, thermal noise is neglected.

We derive the ratio of mean signal power to mean interference power for EGC. For MRC, we determine density functions for the signal-to-interference ratio (SIR) and, in some cases, expressions for the outage and probability of bit error. For optimum combining, we evaluate the SIR density function for the non-fading/Rayleigh and Rayleigh/Rayleigh cases, and closed form expressions of the outage probability and BER in terms of hypergeometric functions. Moreover, we provides a comparison between the various methods.

4.1 Equal Gain Combining

With EGC, each channel is provided with phase compensation to match the phase shift in the channel (the phase is measured with respect to the reference antenna element). All channels are provided with equal gain (without loss of generality, the gain is taken equal to unity). EGC is an attractive method due to its relative ease of implementation.

The method was investigated by several authors. Jakes provided an expression for the SNR in the case of Rayleigh fading [11]. In [14], the cumulative density function of the SNR is evaluated by a series method for Rayleigh and Nakagami channels. This work is extended to Ricean channels in [16]. Here, we briefly study the EGC performance in the presence of CCI. The cases treated are of a desired signal subject to Rayleigh or Ricean fading and CCI subject to Rayleigh fading. These cases are referred to as Rayleigh/Rayleigh and Rice/Rayleigh, respectively. While with MRC and OC performance is evaluated by regarding the SIR as a random variable and characterizing its density function, with EGC our scope was limited to providing an expression for the ratio of mean signal power to mean

interference power. This simplification is necessitated by the fact that the desired signal is expressed by a sum of Rayleigh or Rice distributions for which closed-form expressions are not available.

Before the following work, we have to stress again that the interference amplitude is assumed equal for all CCI sources and is given by $\sqrt{P_I}$. This assumption while restrictive, facilitates the derivation of closed-form expressions

The weight provided to the ith branch of the EGC is given by $\xi_i = e^{j\phi_{s,i}}$. The array weight vector is then given by

$$\mathbf{w} = \underline{\boldsymbol{\xi}}_s, \tag{4.1}$$

where $\underline{\boldsymbol{\xi}}_s^T = [\xi_1, \ldots, \xi_N]$. Based on the signal model in Chapter 2.1 ,The pre-detection signal at the array output is given by

$$\begin{aligned} y[k] &= \mathbf{w}^H \mathbf{u}[\mathbf{k}] \\ &= \sqrt{P_s}\underline{\boldsymbol{\xi}}_s^H \mathbf{c}_s z_s[k] + \sqrt{P_I}\sum_{i=1}^{L} \underline{\boldsymbol{\xi}}_s^H \mathbf{c}_i z_i[k] \end{aligned} \tag{4.2}$$

Note that $\underline{\boldsymbol{\xi}}_s^H \mathbf{c}_s = \sum_{i=1}^{N} \alpha_{s,i}$ is a sum of Rayleigh/Rice random variables. It is easy to show that the signal power averaged over *time and fading* is given by

$$S = P_s\left(N\overline{\alpha_s^2} + N(N-1)\,\overline{\alpha_s}^2\right), \tag{4.3}$$

where $\overline{\alpha_s^2} = E\left[\alpha_{s,n}^2\right]$, $\overline{\alpha_s} = E\left[\alpha_{s,n}\right]$. It can be shown that in the Rayleigh case, the mean value of the desired signal's power is given by [11]

$$S = P_s N\left[1 + (N-1)\,\pi/4\right]. \tag{4.4}$$

The interference power is given by,

$$\begin{aligned} I &= E\left[\left|\sqrt{P_I}\sum_{i=1}^{L} \underline{\boldsymbol{\xi}}_s^H \mathbf{c}_i z_i[k]\right|^2\right] \\ &= P_I\,(1-\beta/4)\sum_{i=1}^{L} E\left[\left|\underline{\boldsymbol{\xi}}_s^H \mathbf{c}_i\right|^2\right], \end{aligned} \tag{4.5}$$

where we used $E\left[z_i^2[k]\right] = 1 - \beta/4$. Since $\underline{\boldsymbol{\xi}}_s$ and $\mathbf{c}_i$ are independent,

$$\begin{aligned} E\left[\left|\underline{\boldsymbol{\xi}}_s^H \mathbf{c}_i\right|^2\right] &= \underline{\boldsymbol{\xi}}_s^H E\left[\mathbf{c}_i \mathbf{c}_i^H\right] \underline{\boldsymbol{\xi}}_s \\ \underline{\boldsymbol{\xi}}_s^H \underline{\boldsymbol{\xi}}_s &= N. \end{aligned} \tag{4.6}$$

Hence,

$$I = P_I\,(1-\beta/4)\,LN. \tag{4.7}$$

Thus the ratio of mean signal power to mean interference power for the Rayleigh/Rayleigh case (Rayleigh desired signal/Rayleigh CCI) is given by

$$\mu_r = \frac{1+(N-1)\,\pi/4}{L}\gamma, \tag{4.8}$$

where γ was defined previously. When the desired signal is subject to the Rice distribution, we have [38]:

$$\overline{\alpha_s} = e^{-K}\Gamma\left(\frac{3}{2}\right){}_1F_1\left(\frac{3}{2},1,K\right) \tag{4.9}$$

and

$$\begin{aligned}\overline{\alpha_s^2} &= e^{-K}{}_1\tilde{F}_1\,(2,1,K)\\ &= (1+K),\end{aligned} \tag{4.10}$$

where $\Gamma\left(\frac{3}{2}\right) = \frac{1}{2}\sqrt{\pi}$, and ${}_1F_1$ denotes the confluent hypergeometric function. Expression (4.9) can be evaluated numerically and substituted back in (4.3). A simple approximation exists for large K [39],

$${}_1F_1\,(a,b,K) \cong \frac{\Gamma\,(b)}{\Gamma\,(a)}\frac{e^K}{K^{b-a}}, \tag{4.11}$$

where Γ is the standard gamma function. Applying (4.11) in (4.9), (4.10) and in (4.3), we obtain for large K:

$$S \cong P_s N^2. \tag{4.12}$$

The EGC ratio of mean signal power to mean interference power for the Ricean signal with large K (non-fading signal) and Rayleigh CCI is then

$$\mu_r \cong \frac{N}{L}\gamma. \tag{4.13}$$

It is observed that this ratio is proportional to the number of antennas and inversely proportional to the number of interference sources.

4.2 Maximal Ratio Combining

When the antennas outputs are combined according to MRC, it is possible to determine the density function of the output SIR in closed-form. The MRC weights are given by [38]:

$$\mathbf{w} = \mathbf{c}_s. \tag{4.14}$$

The output of the combiner is then given by

$$\begin{aligned}y[k] &= \mathbf{w}^H\mathbf{u}[k]\\ &= \sqrt{P_s}\,|\mathbf{c}_s|^2\,z_s[k] + \sqrt{P_I}\sum_{i=1}^{L}\mathbf{c}_s^H\mathbf{c}_i z_i[k].\end{aligned} \tag{4.15}$$

It follows that the frame SIR is

$$\mu = \frac{\gamma \left|\mathbf{c}_s\right|^4}{\sum_{i=1}^{L} \left|\mathbf{c}_s^H \mathbf{c}_i\right|^2}. \tag{4.16}$$

The analysis of MRC consists of the following steps: (1) evaluate the density function of μ (the SIR is a random variable with a range determined by the random vectors $\mathbf{c}_s$, $\mathbf{c}_i$), (2) evaluate the outage probability averaged over outcomes of μ, (3) make the Gaussian assumption with respect to the interference and express the BER conditional on the SIR μ, (4) evaluate the performance averaged over outcomes of μ. The analysis is carried out for the Rayleigh/Rayleigh and Rice/Rayleigh cases. Unless stated otherwise, expressions developed in this section hold for an arbitrary number of antennas and interference sources.

Equation (4.16) can be rewritten

$$\mu = \gamma \frac{\left|\mathbf{c}_s\right|^2}{\sum_{i=1}^{L} \left|\nu_i\right|^2}, \tag{4.17}$$

where $\nu_i = \mathbf{c}_s^H \mathbf{c}_i / \left|\mathbf{c}_s\right|$. We claim that ν_i and $\mathbf{c}_s$ are independent . The interference is assumed subject to Rayleigh distribution, hence the elements of $\mathbf{c}_i$ are i.i.d., zero-mean, complex Gaussian. It follows that the distribution of ν_i conditioned on $\mathbf{c}_s$, is also complex Gaussian. The mean and the variance of the random variable ν_i conditioned on $\mathbf{c}_s$ are respectively

$$E\left[\nu_i \mid \mathbf{c}_s\right] = \frac{\mathbf{c}_s^H}{\left|\mathbf{c}_s\right|} E\left[\mathbf{c}_i\right] = 0, \tag{4.18}$$

and

$$\begin{aligned} E\left[\left|\nu_i\right|^2 \mid \mathbf{c}_s\right] &= \frac{\mathbf{c}_s^H E\left[\mathbf{c}_i \mathbf{c}_i^H\right] \mathbf{c}_s}{\left|\mathbf{c}_s\right|^2} \\ &= \frac{\mathbf{c}_s^H \mathbf{I}_N \mathbf{c}_s}{\left|\mathbf{c}_s\right|^2} \\ &= 1. \end{aligned} \tag{4.19}$$

The density of ν_i conditioned on $\mathbf{c}_s$ can be written $f_{\nu_i}\left(\nu_i \mid \mathbf{c}_s\right) = \pi^{-1} e^{-\left|\nu_i\right|^2}$. It is clear from this expression that ν_i is independent of $\mathbf{c}_s$. The term $\left|\mathbf{c}_s\right|^2 / \sum_{i=1}^{L} \left|\nu_i\right|^2$ in (4.17) is the ratio of independent random variables and it can be written

$$\zeta = \frac{\sum_{j=1}^{N} \left|\, c_{s,j} \,\right|^2}{\sum_{i=1}^{L} \left|\, \nu_i \,\right|^2} \tag{4.20}$$

where $\mathbf{c}_s = \left[c_{s,1}, \ldots, c_{s,N}\right]^T$.

For Rayleigh/Rayleigh (signal/CCI) fading and since each of $C_{S,J}$ and ν_i are complex Gaussian random variables, $2\left|\, c_{s,j} \,\right|^2$ and $2\left|\nu_i\right|^2$ are central chi-square random variables with 2 degrees of freedom. The quantity $\zeta = \sum_{j=1}^{N} \left|\, c_{s,j} \,\right|^2 / \sum_{i=1}^{L} \left|\nu_i\right|^2$ is recognized as the ratio of two independent central chi-square random variables; the numerator with $2N$ degrees of

freedom and the denominator with $2L$ degrees of freedom. The distribution of ζ is therefore given by [40]

$$f_\zeta(\zeta) = \frac{\Gamma(L+N)}{\Gamma(L)\Gamma(N)} \frac{\zeta^{N-1}}{(1+\zeta)^{L+N}} \tag{4.21}$$

for $\zeta \geq 0,\ N \geq 1,\ L \geq 1$. The density in (4.21) is a modified form of the central F distribution. The term 'modified' refers to the fact that the ratio of two independent central chi-squared random variables normalized by their respective degrees of freedom has a central F distribution, while in this case the random variables are not normalized. It is observed that $\zeta \sim \frac{N}{L}F$,where F denotes the F distribution. By using the transformation of variables $\mu = \gamma\zeta$, the density of the SIR μ can easily be obtained and is

$$f_\mu(\mu) = \frac{\Gamma(L+N)}{\Gamma(L)\Gamma(N)} \gamma^L \frac{\mu^{N-1}}{(\gamma+\mu)^{L+N}}. \tag{4.22}$$

To reiterate, this expression applies only to equal-power interferers. The mean SIR is given by

$$\begin{aligned} \overline{\mu} &= \frac{\Gamma(L+N)}{\Gamma(L)\Gamma(N)} \gamma^L \int_0^\infty \frac{\mu^N}{(\gamma+\mu)^{L+N}} d\mu \\ &= \frac{N}{L-1}\gamma, \end{aligned} \tag{4.23}$$

where $L > 1$. The mean SIR is proportional to the number of elements N and inverse proportional to the number of interference sources L.

When the desired signal is subject to the Rice distribution, the terms $c_{s,j}$ in (4.20) are distributed as $\mathcal{CN}\left(\sqrt{K}, 1\right)$. Hence, the distribution of $2|\ c_{s,j}\ |^2$ is non-central chi-square with 2 degrees of freedom and parameter K. In the appendix it is shown that the distribution of ζ in (4.20) is given by,

$$\begin{aligned} f_\zeta(\zeta) &= e^{-NK}{}_1F_1\left(L+N, N; NK\frac{\zeta}{1+\zeta}\right) \\ &\quad \frac{\Gamma(L+N)}{\Gamma(L)\Gamma(N)} \frac{\zeta^{N-1}}{(1+\zeta)^{L+N}}. \end{aligned} \tag{4.24}$$

The density function of the SIR can now be obtained from (4.24) and the relation $\mu = \gamma\zeta$,

$$\begin{aligned} f_\mu(\mu) &= e^{-NK}{}_1F_1\left(L+N, N; NK\frac{\mu}{\gamma+\mu}\right)\gamma^L \\ &\quad \frac{\Gamma(L+N)}{\Gamma(L)\Gamma(N)} \frac{\mu^{N-1}}{(\gamma+\mu)^{L+N}}. \end{aligned} \tag{4.25}$$

When $K = 0$, the relation above degenerates to the Rayleigh distribution case. When $K \to \infty$, i.e., the desired signal is non-fading (non-fading/Rayleigh case), and the appropriate quantities are substituted in (4.16), the SIR at the output of the MRC can be expressed as

$$\mu = \gamma \frac{N^2}{\mathbf{c}_s^H \mathbf{S} \mathbf{c}_s}, \tag{4.26}$$

where $\mathbf{c}_s = \left[1, e^{j\phi_{s,2}} \ldots, e^{j\phi_{s,N}}\right]$, $\mathbf{c}_s^H \mathbf{c}_s = N$, and $\mathbf{S} = \sum_{i=1}^{L} \mathbf{c}_i \mathbf{c}_i^H$. The matrix $\mathbf{S}$ has a complex Wishart distribution $\mathcal{CW}_N(\mathbf{I}_N, L)$ [41]. The distribution of $\zeta = \mathbf{c}_s^H \mathbf{S} \mathbf{c}_s$ is $\mathcal{CW}_1(N, L)$ [40], which is just the exponential distribution

$$f_\zeta(\zeta) = \frac{N^{-L}}{\Gamma(L)} \zeta^{L-1} e^{-\zeta/N}. \tag{4.27}$$

It follows that the distribution of the SIR $\mu = \gamma N^2/\zeta$ is expressed by

$$f_\mu(\mu) = \frac{(N\gamma)^L}{\Gamma(L)} \mu^{-L-1} e^{-N\gamma/\mu}. \tag{4.28}$$

Computation of the mean value of the SIR in the non-fading/Rayleigh case reveals that it is the same as in the Rayleigh/Rayleigh case, i.e.,

$$\overline{\mu} = \frac{N}{L-1}\gamma. \tag{4.29}$$

4.2.1 Outage Probability

The outage is defined as the probability of failing to achieve a prescribed SIR:

$$P_o = \Pr\left[\mu < \mu_p\right], \tag{4.30}$$

where μ_p is the desired SIR threshold. A suitable threshold level depends on the modulation technique used and performance desired [42]. For the Rayleigh/Rayleigh and non-fading/Rayleigh cases, the outage can be found in closed-form. For the Rayleigh/Rayleigh case, the outage is then given by,

$$\begin{aligned} P_o &= \int_0^{\mu_p} f_\mu(\mu) d\mu \\ &= \frac{\Gamma(L+N)}{\Gamma(L)\Gamma(N)} \gamma^L \int_0^{\mu_p} \frac{\mu^{N-1}}{(\gamma+\mu)^{L+N}} d\mu. \end{aligned} \tag{4.31}$$

Equation (4.31) can be evaluated in a closed-form using integral tables [43]:

$$P_o = \frac{\Gamma(L+N)}{\Gamma(L)\Gamma(N+1)} \left(\frac{\mu_p}{\gamma}\right)^N {}_2F_1\left(L+N, N; N+1; -\frac{\mu_p}{\gamma}\right), \tag{4.32}$$

where ${}_2F_1(a, b; c; x)$ is the Gauss hypergeometric function [44]. Using (4.28) in (4.31), it is not difficult to show that the outage for non-fading/Rayleigh is given by

$$P_o = \frac{\Gamma(L, N\gamma/\mu_p)}{\Gamma(L)}, \tag{4.33}$$

where $\Gamma(L, x) = \int_x^\infty t^{L-1} e^{-t} dt$, is the incomplete gamma function [44].

4.2.2 Average Probability of Error

The computation of the probability of error is based on the Gaussian assumption for the interference. Specifically, the interference term in (4.15) is assumed to have a Gaussian distribution. The conventional form of the central limit theorem does not formally apply here as the interference term $y_I[k] = \sqrt{P_I}\sum_{i=1}^{L} \mathbf{c}_s^H \mathbf{c}_i z_i[k]$ consists of independent, but not identically distributed terms $\sqrt{P_I}\mathbf{c}_s^H\mathbf{c}_i$. However, a form of the central limit theorem given by Cramer can be applied [45]. Cramer's central limit theorem states that the sum $X_1 + \ldots + X_n$ of a large number of independent variables, is approximately normally distributed if: (i) every component has a zero mean value, (ii) every component has a finite variance $\sigma_i^2 = E\left[|X_i|^2\right]$, and (iii) $\sigma_i/s_n \to 0$ and $s_n \to \infty$, where $s_n = \sigma_1^2 + \ldots + \sigma_n^2$. From the properties of the variable $z_i[k]$ specified following (3.2), it can be easily shown that aggregate interference $y_I[k]$ meets the conditions of the theorem, and hence, it can be assumed Gaussian.

Consequently, the conditional BER is given by

$$P_{e|\mu} = Q(\sqrt{2\mu}), \tag{4.34}$$

where $Q(x) = \frac{1}{\sqrt{2\pi}}\int_x^\infty e^{-t^2/2}\,dt$ is the area under the tail of the Gaussian probability density function. In integral tables used to obtain the results below, the related function erfc$(\cdot)$ (the complementary error function) is usually found ($Q(\sqrt{2x}) = \frac{1}{2}\text{erfc}(\sqrt{x})$). For the Rayleigh/Rayleigh case, using (4.22), the average BER can be written

$$\begin{aligned} P_e &= \frac{1}{2}\int_0^\infty \text{erfc}(\sqrt{\mu}) f_\mu(\mu) d\mu \\ &= \frac{1}{2}\frac{\Gamma(L+N)}{\Gamma(L)\Gamma(N)}\gamma^L \int_0^\infty \text{erfc}(\sqrt{\mu})\frac{\mu^{N-1}}{(\gamma+\mu)^{L+N}} d\mu. \end{aligned} \tag{4.35}$$

An alternative expression to (4.35) in terms of hypergeometric series is given in [46]:

$$\begin{aligned} P_e = \frac{1}{2\sqrt{\pi}\Gamma(L)\Gamma(N)} \Bigg[& \gamma^L \frac{\Gamma(\frac{1}{2}-L)\Gamma(L+N)}{(-L)} \\ & {}_2F_2\left(L+N, L; L+\frac{1}{2}, L+1; \gamma\right) + \gamma^{\frac{1}{2}}\frac{\Gamma(L-\frac{1}{2})}{\Gamma(\frac{1}{2})} \\ & \Gamma(-\frac{1}{2})\Gamma(N+\frac{1}{2}){}_2F_2\left(N+\frac{1}{2}, \frac{1}{2}; \frac{3}{2}-L, \frac{3}{2}; \gamma\right) + \Gamma(L)\Gamma(\frac{1}{2})\Gamma(N)\Bigg], \end{aligned} \tag{4.36}$$

where ${}_2F_2(\cdot)$ is a hypergeometric function. Even though (4.36) looks more involved than (4.35), it might be more convenient for numerical evaluations using a software package such as Mathematica.

For the Rice/Rayleigh case, a closed-form expression could not be found for the average probability of bit error.

4.3 Optimum Combining

With optimum combining, the weight vector that maximizes SIR at the output of the array is [47]

$$\mathbf{w} = \alpha \mathbf{R}^{-1}\mathbf{c}_s, \tag{4.37}$$

where α is an arbitrary constant. The constant α does not affect the SIR at the array output. The interference covariance matrix, conditioned on channel vectors $\mathbf{c}_i$, is

$$\mathbf{R} = \sum_{i=1}^{L} P_i \mathbf{c}_i \mathbf{c}_i^H, \tag{4.38}$$

where the superscript $\{H\}$ stands for transpose complex conjugate. Note that $\mathbf{R}$ varies with the fading rate and that we have assumed that the fading rate is much less than the bit rate.

The vectors $\mathbf{c}_i, i = 1, \ldots, L$, are i.i.d., complex Gaussian with mean $\{E[\mathbf{c}_i] = \mathbf{0}\}$ and covariance matrix $\left\{\Sigma = E\left[\mathbf{c}_i \mathbf{c}_i^H\right]\right\}$. The same parameters hold for $\mathbf{c}_s$. By definition, Σ is positive semidefinite and Hermitian. By assumption, it will be positive definite, hence, its inverse exists. When independent fading at each antenna element is assumed and $\sigma^2 = 1$, then $\Sigma = \mathbf{I}_N$, where $\mathbf{I}_N$ is an identity matrix of dimension N. When $\Sigma > 0$, i.e. positive definite, and $L \geq N$, the matrix $\mathbf{R}$ is positive definite with probability one [48]. Thus, $\mathbf{R}^{-1}$ exists in (4.37). The density of such random matrices was studied in [49]. Therein it is shown that the joint distribution of the elements $\mathbf{R}$ is given by:

$$f_{\mathbf{R}}(\mathbf{R}) = \begin{cases} \frac{|\mathbf{R}|^{L-N}|\Sigma|^{-L}|\Lambda|^{-N}{}_0F_0^{(L)}\left(\Lambda^{-1},-\Sigma^{-1}\mathbf{R}\right)}{\tilde{\Gamma}_N(L)} & \mathbf{R} > 0, \Sigma > 0 \\ 0 & \text{otherwise,} \end{cases} \tag{4.39}$$

where $|\cdot|$ denotes the determinant of a matrix. The complex multivariate gamma function $\tilde{\Gamma}_N(L)$ is defined

$$\tilde{\Gamma}_N(L) = \pi^{\frac{N(N-1)}{2}} \prod_{i=i}^{N} \Gamma(L - i + 1), \tag{4.40}$$

where $\Gamma(\cdot)$ is the standard gamma function. The quantity ${}_0F_0^{(L)}\left(\Lambda^{-1}, \Sigma^{-1}\mathbf{R}\right)$ is a hypergeometric function with matrix arguments [49]. The matrix $\Lambda = \text{diag}\,(P_1, \ldots, P_L)$. For the special case of $P_i = P_I$, i.e., all interferers have equal-power P_I, the density function in (4.39) reduces to the complex Wishart distribution

$$f_{\mathbf{R}}(\mathbf{R}) = \begin{cases} \frac{|\mathbf{R}|^{L-N}|\Sigma|^{-L}e^{-\text{tr}\left(\frac{1}{P}\Sigma^{-1}\mathbf{R}\right)}}{\tilde{\Gamma}_N(L)P^{LN}} & \mathbf{R} > 0, \Sigma > 0 \\ 0 & \text{otherwise,} \end{cases} \tag{4.41}$$

where $\text{tr}(\cdot)$ denotes the trace of a matrix. In deriving (4.41) from (4.39), we have used the following relations [50]:

$$\begin{aligned} {}_0F_0^{(L)}\left(\Lambda^{-1}, -\Sigma^{-1}\mathbf{R}\right) &= {}_0F_0^{(L)}\left(P_I^{-1}\mathbf{I}, -\Sigma^{-1}\mathbf{R}\right) \\ &= {}_0F_0^{(L)}\left(\mathbf{I}, -P_I^{-1}\Sigma^{-1}\mathbf{R}\right) \\ &= {}_0F_0\left(-P_I^{-1}\Sigma^{-1}\mathbf{R}\right) \\ &= e^{-\text{tr}\left(P^{-1}\Sigma^{-1}\mathbf{R}\right)} \end{aligned} \tag{4.42}$$

The distribution in (4.41) (apart from a constant factor) is the complex Wishart distribution with parameter Σ and L degrees of freedom. It is denoted as $\text{CW}_N(\Sigma, L)$. The Wishart distribution is the multivariate generalization of the chi-square distribution [50].

4.3.1 Density of Maximum SIR for non-fading/Rayleigh Case

For the Rice/Rayleigh and case, the SIR at the output of the optimum combiner is given by $\mu = \gamma\zeta$, where

$$\zeta = \mathbf{c}_s^H \left(\mathbf{C}\mathbf{C}^H\right)^{-1} \mathbf{c}_s, \tag{4.43}$$

and $\gamma = P_s/\left(P_I\left(1-\beta/4\right)\right)$. The vector $\mathbf{c}_s$ has a multivariate distribution which is given by $\mathcal{CN}_N\left(\sqrt{K}\mathbf{1}_N, \mathbf{I}_N\right)$, while the columns of $\mathbf{C}\{[\mathbf{c}_1, \ldots, \mathbf{c}_L]\}$ have a distribution which is given by $\mathcal{CN}_N\left(\mathbf{0}_N, \mathbf{I}_N\right)$, where $\mathbf{0}_N$ is a vector of zeros of dimension N. The density of ζ can be found according to [40]. After a suitable transformation, we obtain

$$\begin{aligned} f_\mu(\mu) &= e^{-NK}{}_1F_1\left(L+N, N; NK\frac{\mu}{\gamma+\mu}\right)\gamma^{L+1-N} \\ &\quad \frac{\Gamma(L+1)}{\Gamma(L+1-N)\Gamma(N)}\frac{\mu^{N-1}}{(\gamma+\mu)^{L+1}}, \end{aligned} \tag{4.44}$$

where the expression holds for a number of CCI sources $L \geq N$. Note the similarities and differences between this expression and (4.25); both have a modified non-central F distribution, but with different degrees of freedom.

In the non-fading/Rayleigh case, the SIR at the output of the optimum combiner is given by

$$\mu = \gamma \mathbf{c}_s^H \mathbf{S}^{-1} \mathbf{c}_s, \tag{4.45}$$

where $\mathbf{S} = \mathbf{C}\mathbf{C}^H$. To determine the SIR density at the output of the optimum combiner, first note that $\mathbf{S}$ has a complex Wishart distribution $\mathcal{CW}_N(\mathbf{I}, L)$. The distribution of ζ^{-1} is then $\mathcal{CW}_1(1/N, L+1-N)$ [40]. Then,

$$f_\zeta(\zeta) = \frac{N^{L+1-N}}{\Gamma(L+1-N)}\zeta^{N-L-2}e^{-N/\zeta}. \tag{4.46}$$

It follows that

$$f_\mu(\mu) = \frac{(N\gamma)^{L+1-N}}{\Gamma(L+1-N)}\mu^{N-L-2}e^{-N\gamma/\zeta}. \tag{4.47}$$

The mean value SIR for the non-fading/Rayleigh case is computed to be

$$\overline{\mu} = \frac{N}{L-N}\gamma. \tag{4.48}$$

4.3.2 Density of Maximum SIR for Rayleigh/Rayleigh Case

Using (4.37), the maximum SIR for Rayleigh/Rayleigh case at the array output can be easily computed and is given by

$$\mu = P_s \mathbf{c}_s^H \mathbf{R}^{-1} \mathbf{c}_s, \tag{4.49}$$

where $\mathbf{R}$ is as defined in (4.38). Since the channel $\mathbf{c}_s$ and the CCI covariance matrix $\mathbf{R}$ are both random, the SIR μ is a random variable. Such random variables for the general case of arbitrary interference powers P_i were studied in [49]. It is shown that the density is given in terms of the hypergeometric function ${}_1F_0$ with matrix arguments:

$$f_\mu(\mu) = \frac{\Gamma(L+1)}{\Gamma(N)\Gamma(L+1-N)} \frac{\mu^{N-1}\beta^{L+1}}{(1+\beta\mu)^{L+1}} |\Lambda|^{-N} {}_1F_0^{(L)}(L+1;\mathbf{Y};\mathbf{Z}), \tag{4.50}$$

where $\beta > 0$ is a constant, and ${}_1F_0^{(L)}(L+1;\mathbf{Y};\mathbf{Z})$ is a hypergeometric function of matrix arguments. The constant β is such that the zonal polynomial series for the ${}_1F_0^{(L)}$ function converges for all $\mathbf{Z}$. The matrices $\mathbf{Y} = \mathbf{I}_L - \beta\Lambda^{-1}$ and $\mathbf{Z} = \mathrm{diag}\big((1+\beta\mu)^{-1}, \mathbf{I}_{N-1}\big)$. Details on the theory of zonal polynomials can be found in [49, 51]. Further analysis of this general case fails to gain insight into the performance of such systems due to the conditioning of $f_\mu(\mu)$ on the powers of individual CCI (through matrix Λ) and the complexity of the theory for this general case. This motivates to continue the analysis with the special case equal-power interferers.

The covariance matrix $\mathbf{R}$, in the case of equal-power interferers is

$$\mathbf{R} = P_I \sum_{i=1}^{L} \mathbf{c}_i \mathbf{c}_i^H. \tag{4.51}$$

Let $\mathbf{R} = P_I \mathbf{R}_1$, where $\mathbf{R}_1 = \sum_{i=1}^{L} \mathbf{c}_i \mathbf{c}_i^H$. The maximum SIR μ is

$$\mu = P_s \mathbf{c}_s^H \mathbf{R}^{-1} \mathbf{c}_s = \frac{P_s}{P_I} \mathbf{c}_s^H \mathbf{R}_1^{-1} \mathbf{c}_s = \frac{P_s}{P_I} \nu, \tag{4.52}$$

where the real scalar quantity $\nu = \mathbf{c}_s^H \mathbf{R}_1^{-1} \mathbf{c}_s$. Since $\mathbf{c}_s$ is complex Gaussian with mean $\mathbf{0}$, covariance matrix Σ, and it is distributed independently of $\mathbf{R}_1$ which is $CW_N(\Sigma, L)$, the density of ν is [40, 49]

$$f_\nu(\nu) = \frac{\Gamma(L+1)}{\Gamma(N)\Gamma(L+1-N)} \frac{\nu^{N-1}}{(1+\nu)^{L+1}} \qquad \nu \geq 0,\ 1 \leq N \leq L. \tag{4.53}$$

The distribution in eq. (4.53) is a modified form of the central F distribution. In multivariate statistics, when the elements of $\mathbf{c}_i$ are real Gaussian with zero means and σ^2 variances, and the elements of $\mathbf{c}_s$ are real Gaussian with arbitrary means and σ^2 variances, then ν (apart from a constant) is known as the Hotelling's T^2 statistic [50]. When $\mathbf{c}_s$ and $\mathbf{c}_i$ have the same mean vector $\mathbf{0}$ and the same covariance matrix Σ, the distribution of ν is known as the *Null* distribution of the Hotelling's T^2 statistic [52]. By using the transformation $\mu = \frac{P_s}{P_I}\nu$, the density of the maximum SIR μ can easily be obtained and is

$$f_\mu(\mu) = \frac{\Gamma(L+1)}{\Gamma(N)\Gamma(L+1-N)} \left(\frac{P_s}{P_I}\right)^{L+1-N} \frac{\mu^{N-1}}{(\frac{P_s}{P_I}+\mu)^{L+1}} \qquad \mu \geq 0,\ 1 \leq N \leq L. \tag{4.54}$$

It is important to note that the density of μ does not depend on the form of the covariance matrix Σ. In other words, the performance of the optimum combiner is the same regardless

whether the fading at the receiver antenna elements is independent or not. This is, however, only true for $L \geq N$ and equal-power interferers.

Further insight can be obtained by calculating the mean SIR $E[\mu]$. We have,

$$\begin{aligned} E[\mu] &= \frac{\Gamma(L+1)}{\Gamma(N)\Gamma(L+1-N)}\left(\frac{P_s}{P_I}\right)^{L+1-N}\int_0^\infty \frac{\mu^N}{(\frac{P_s}{P_I}+\mu)^{L+1}}d\mu \\ &= \frac{N}{L-N}\frac{P_s}{P_I} \qquad 1 \leq N < L. \end{aligned} \tag{4.55}$$

It should be noted that the integral involved in the computation of $E[\mu]$ does not exist for $L = N$. For a number of CCI's L much larger than the number of antennas N, the mean SIR is proportional to N.

4.3.3 Outage Probability

Probability of outage is an important statistical measure in the design of cellular mobile radio systems which operate in a fading environment with multiple interferers [53]. It represents the probability of unsatisfactory reception over the intended coverage area. A system planner can use outage probability calculations to assess the effects of various system configurations on the quality of service provided by the system. The outage probability is defined as the probability of failing to achieve a SIR sufficient to give satisfactory radio reception and is expressed as

$$\begin{aligned} P_o &= \text{Probability}\left[\mu < \mu_p\right] \\ &= \int_0^{\mu_p} f_\mu(\mu)d\mu \\ &= \frac{\Gamma(L+1)}{\Gamma(N)\Gamma(L+1-N)}\left(\frac{P_s}{P_I}\right)^{L+1-N}\int_0^{\mu_p}\frac{\mu^{N-1}}{(\frac{P_s}{P_I}+\mu)^{L+1}}d\mu, \end{aligned} \tag{4.56}$$

where μ_p is the SIR protection ratio which depends on the modulation technique used and performance desired. In other words, the outage probability is the cumulative distribution function. Equation (4.56) can be evaluated as the following infinite series form [54] and is

$$P_o = \frac{\Gamma(L+1)}{\Gamma(N+1)\Gamma(L+1-N)}\left(\frac{\mu_p P_I}{P_s}\right)^N {}_2F_1\left(L+1, N; N+1; -\frac{\mu_p P_I}{P_s}\right), \tag{4.57}$$

where ${}_2F_1(a, b; c; x)$ is the hypergeometric function defined as [55]

$${}_2F_1(a, b; c; x) = \sum_{n=0}^{\infty}\frac{(a)_n(b)_n}{(c)_n}\frac{x^n}{n!}. \tag{4.58}$$

The notation $(\cdot)_n$ is called the Pochhammer symbol and is defined as $(a)_n = \frac{\Gamma(a+n)}{\Gamma(a)}$. The infinite series in (4.57) is convergent.

4.3.4 Average BER

As mentioned earlier, subsequent to Rayleigh fading, the in-phase and quadrature components of each of the received cochannel interferers have a Gaussian distribution. That is, each of the quantities $\sqrt{P_I}\mathbf{c}_i s_i(t)$, $i = 1, \ldots, L$, has a complex Gaussian distribution. The sum of the interferers is also complex Gaussian. Since the optimum combiner is a linear filter, the sum of the interferers at the output of the optimum combiner (antenna array) is also complex Gaussian. Thus, the conditional BER, i.e., the BER computed for a given value of μ, is simply

$$P_{e|\mu} = Q(\sqrt{2\mu}),$$

where $Q(\cdot)$ is the area under the tail of the Gaussian probability density function and is defined as

$$Q(x) = \frac{1}{\sqrt{2\pi}} \int_x^\infty e^{-t^2/2}\, dt. \tag{4.59}$$

In integral tables used to obtain the results below, the related function $\text{erfc}(\cdot)$ (the complementary error function) is usually found. The relation between the two functions is $Q(\sqrt{2x}) = \frac{1}{2}\text{erfc}(\sqrt{x})$.The average BER, i.e., the one averaged over all the values of μ is

$$\begin{aligned} P_e &= \frac{1}{2}\int_0^\infty \text{erfc}(\sqrt{\mu}) f_\mu(\mu) d\mu \\ &= \frac{1}{2}\frac{\Gamma(L+1)}{\Gamma(N)\Gamma(L+1-N)}\left(\frac{P_s}{P_I}\right)^{L+1-N} \int_0^\infty \text{erfc}(\sqrt{\mu}) \frac{\mu^{N-1}}{(\frac{P_s}{P} + \mu)^{L+1}} d\mu. \end{aligned} \tag{4.60}$$

As shown in the appendix, (4.60) can be evaluated as

$$\begin{aligned} P_e \;=\; & \frac{1}{2\sqrt{\pi}\Gamma(N)\Gamma(L+1-N)} \left[\left(\frac{P_s}{P_I}\right)^{L+1-N} \frac{\Gamma(N-L-\frac{1}{2})\Gamma(L+1)}{(N-L-1)} \right. \\ & {}_2F_2\left(L+1, L+1-N; L-N+\frac{3}{2}, L-N+2; \frac{P_s}{P_I}\right) + \left(\frac{P_s}{P_I}\right)^{\frac{1}{2}} \frac{\Gamma(L-N+\frac{1}{2})}{\Gamma(\frac{1}{2})} \\ & \left. \Gamma(-\frac{1}{2})\Gamma(N+\frac{1}{2}) {}_2F_2\left(N+\frac{1}{2}, \frac{1}{2}; N-L+\frac{1}{2}, \frac{3}{2}; \frac{P_s}{P_I}\right) + \frac{\Gamma(L+1-N)\Gamma(\frac{1}{2})\Gamma(N)}{\Gamma(1)} \right], \end{aligned} \tag{4.61}$$

where ${}_pF_q(\cdot)$ is the generalized hypergeometric series and is defined as [55]

$${}_pF_q\left(a_1, \ldots, a_p; b_1, \ldots, b_q; x\right) = \sum_{n=0}^{\infty} \frac{(a_1)_n \cdots (a_p)_n}{(b_1)_n \cdots (b_q)_n} \frac{x^n}{n!}. \tag{4.62}$$

Equation (4.61) can be evaluated using software packages such as Maple, Mathematica, etc. Alternatively, (4.60) can be evaluated numerically.

4.4 Numerical Results

In this section numerical results are presented on the performance of MRC and OC. Performance is evaluated for 6 or 18 equal-power interference sources subject to independent Rayleigh fading. A reminder, in all figures, SIR is to be understood as the frame SIR and the quantity γ is defined as $\gamma = P_s/P_I/(1-\beta/4)$. Unless specified otherwise, $\beta = 0$ and $P_s/P_I = 1$.

In Figures 4.1-4.6 the SOI and CCI are subject to Rayleigh fading. In Figure 4.1, the density function of the frame SIR measured at the array output is plotted for $L = 6$ interference sources, with the number of antenna elements N as the parameter. These curves clearly show that the SIR has a better chance to take on high values with the increase in the order of diversity N, regardless of the combining method. Note that OC significantly increases the chances of higher SIR values, as compared to MRC. For $N = 1$, both MRC and OC provide identical results, as expected. In Figure 4.2, the density functions of the frame SIR obtained by both theory and Monte Carlo simulations are compared for the case of $L = 6$ interference sources. These curves show a very good match between the theory and simulations. Figure 4.3 shows the outage probability versus the channel SIR γ with the number of antennas N as the parameter. The figure shows the case of $L = 6$ interference sources and $\beta = 0$ excess bandwidth. For a given γ, OC decreases the outage probability as compared to MRC and this decrease becomes even greater as N increases. For a given outage probability, increasing N reduces the required γ, subsequently enabling an increase in the number of users. In Figure 4.4, the average probability of bit error is plotted versus the channel SIR γ. The curves represent theory and simulations results for $L = 18$ interference sources. The BER shown accounts for SOI and CCI subject to Rayleigh fading as expressed by (4.36) for MRC and by the results in [1] for OC. Figure 4.5 provides the average probability of bit error as a function of the channel SIR γ for two values of the number of antennas. It is observed that OC can provide improved BER even in the case when the number of interference sources $L = 18$ is much larger than the number of antennas. For example, for a BER of 10^{-3} and $N = 6$, OC requires 1 dB less input SIR than MRC. Figure 4.6 shows the improvement, due to OC versus the average probability of bit error with the number of elements N as the parameter. The improvement is defined as the reduction in the required input SIR per channel γ, to obtain a given BER using OC and compared to MRC. The improvement increases with N and slowly decreases with decreasing BER for a given N.

Figures 4.7-4.8 show the effect of the SOI subject to Ricean fading or non-fading. The curves represent the case of $N = 4$ antenna elements and $L = 6$ interference sources. In Figure 4.7, the density functions of the frame SIR are plotted for MRC and OC for the Rice/Rayleigh case. The density functions are given by (4.25) for MRC and by (4.44) for OC. The SOI is subject to Ricean fading with parameter $K = 5$. Figure 4.8 contains curves of the density functions of the frame SIR for MRC and OC for the non-fading/Rayleigh case, as given by expressions (4.28) and (4.47), respectively. The curves represent the case of $N = 4$ antenna elements and $L = 6$ interference sources.

Meantime, we present the results on the performance of the array with optimum combining studied in the previous sections . We evaluate the system performance for the worst case scenario only, i.e., the mobile transmitting the desired signal is at the point in the cell farthest from the base station, and the interfering mobiles in the surrounding cells are as

close as possible to the base station of the desired mobile. Furthermore, we consider only the six strongest interferers ($L = 6$), i.e., interferers from the first tier of cochannel cells. This is a reasonable assumption as the interference from the second tier of cochannel cells is negligible. As explained in the introduction, we make the assumption of equal-power interferers. Due to this assumption, the results are pessimistic with respect to the case of unequal-power when the largest interferer is of the same power as the ones assumed here. The variance σ^2 of the channel coefficients was assumed 1.

In Figure 4.9, the probability density function of the maximum SIR μ is plotted, with the number of antenna elements N as the parameter. This curve clearly show that the maximum SIR μ has a better chance to take on large values as N increases. In Figure 4.10, the densities obtained by both the theory (eq. (4.54)) and Monte Carlo simulations are compared. Simulations were carried out using MATLAB software. The channel vectors were assumed constant over one bit interval and independent between different bit intervals. The number of samples used in the Monte Carlo simulations was 200,000. A very good match between the theory and simulations is evident from the figure.

Figure 4.11 shows the outage probability versus P_s/P_I with N as the parameter. For a given outage probability, increasing N reduces the required P_s/P_I, subsequently increasing the number of users.

In Figure 4.12, the BER is plotted versus P_s/P_I with N as the parameter. For a given BER, increasing N reduces the required P_s/P_I, which in turn, leads to an increase in the system capacity.

Figure 4.13 shows the diversity gain due to optimum combining versus the number of antenna elements N. The diversity gain is defined as the reduction in the required P_s/P_I, for a given BER, with a corresponding increase in N.

It should be noted that the results provided here are for the worst case scenario, and hence, pessimistic. In a real system, the performance of the optimum combiner can be expected to be far better than the one shown in this paper due to the following: first, due to random locations of the mobiles, the total received interference power will be lower than in the worst case assumed here, second, all channels in all cells may not always be occupied, reducing the total interference.

4.5 Discussion

In this chapter, we studied and compared the performance of digital cellular mobile radio communication systems employing antenna arrays utilizing various forms of combining the outputs: MRC, OC, and EGC. The problem addressed was the detection of a BPSK signal in the presence of multiple CCI sources in a quasi-static, flat fading environment. The analysis considered Rayleigh or Rice fading of the SOI and Rayleigh fading for the CCI. For EGC, expressions were derived for the ratio of mean signal power to mean interference power for Rayleigh and Rice fading. For MRC, analytical expression were obtained for the density function of the SIR, the average outage probability and the average probability of bit error. For OC, the density function of the SIR, the average outage probability and the average probability of bit error were obtained for Rice fading and Rayleigh fading.

All results were obtained under the assumption of equal power CCI sources. For MRC, the results hold for an arbitrary number of interference sources, while for OC the number of sources is larger or equal to the number of antennas. In this case, the array degrees of freedom are not sufficient to null the interference sources and thus fading of the interference has a significant impact on performance. The analytical expressions derived in the paper facilitate the comparison of MRC and OC and demonstrate the advantage of OC even when the number of CCI sources exceeds the number of antennas.

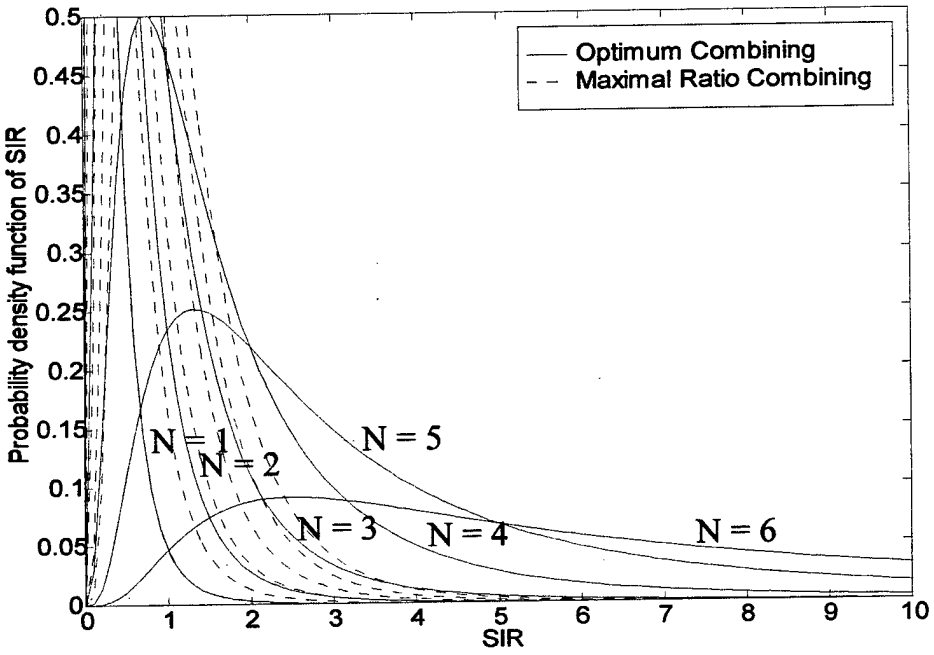

Figure 4.1: Probability density function of the frame SIR for $L = 6$ interference sources, Rayleigh/Rayleigh fading.

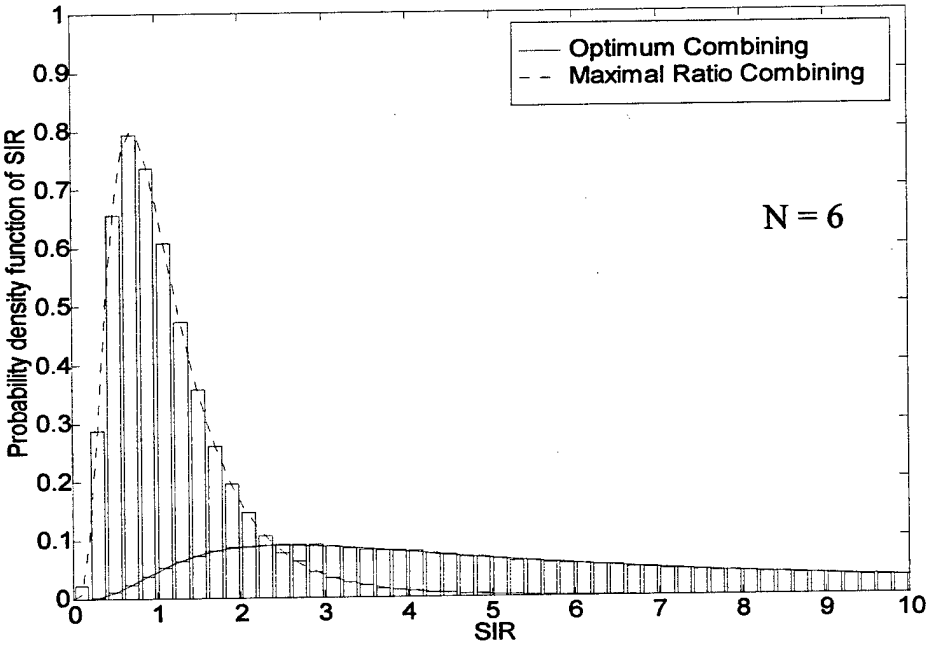

Figure 4.2: Theory and simulation, optimum combining and maximal ratio combining, for $L = 6$ interference sources, Rayleigh/Rayleigh fading.

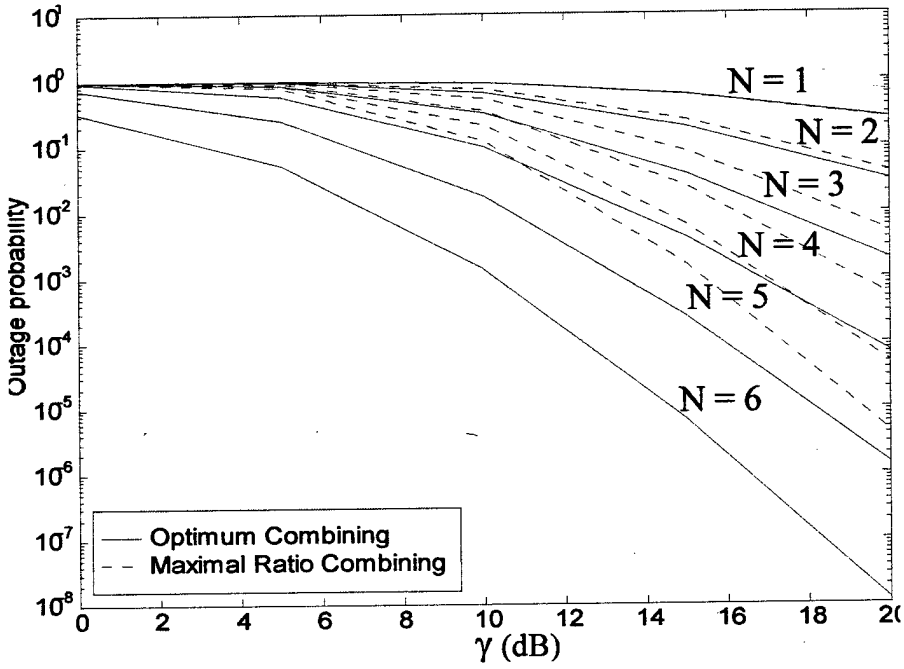

Figure 4.3: The outage probability versus γ with the order of diversity N as the parameter for $L = 6$ interference sources, Rayleigh/Rayleigh fading.

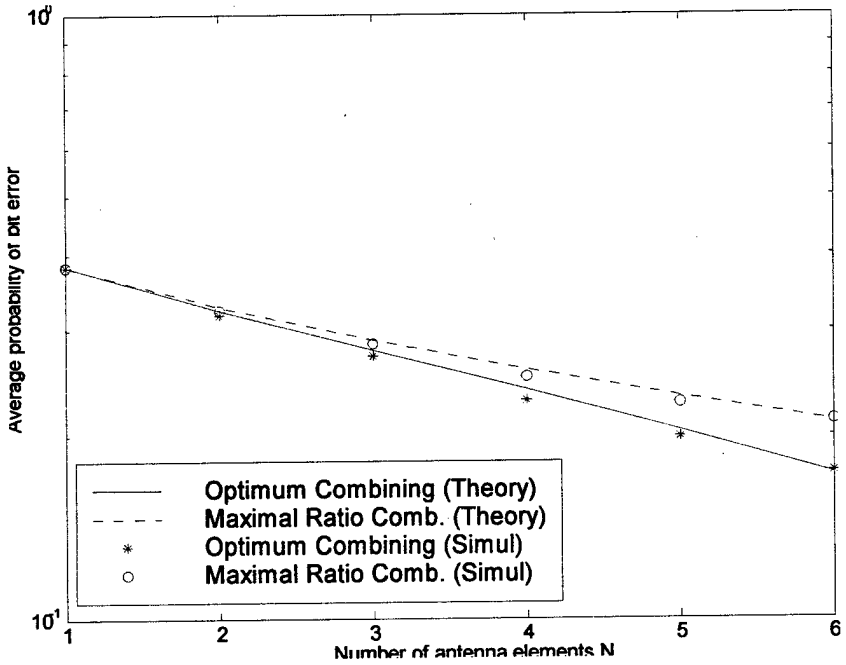

Figure 4.4: Theory and simulation: average probability of bit error versus number of antennas for $L = 18$ interference sources, Rayleigh/Rayleigh fading.

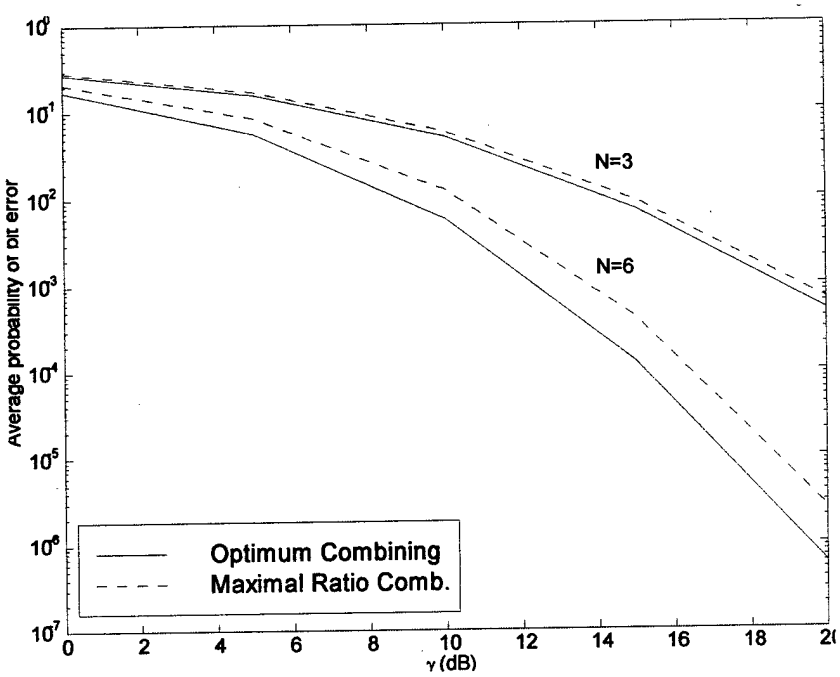

Figure 4.5: Bit error rate versus SIR for $L = 18$ interference sources, Rayleigh/Rayleigh fading.

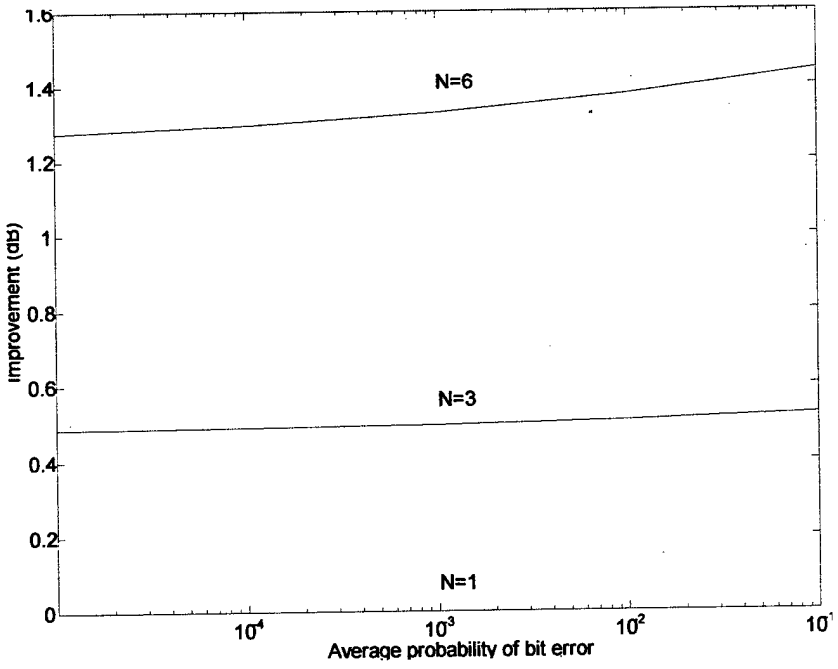

Figure 4.6: Improvement of OC over MRC for $L = 18$ interference sources, Rayleigh/Rayleigh fading.

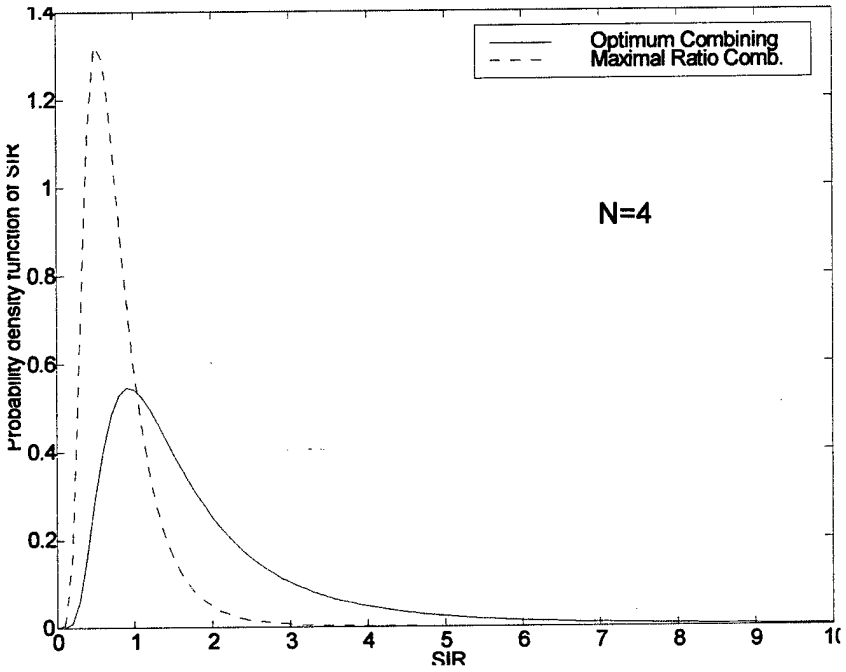

Figure 4.7: Density function of the frame SIR for $L = 6$ interference sources, Rice/Rayleigh fading with Ricean parameter $K = 5$.

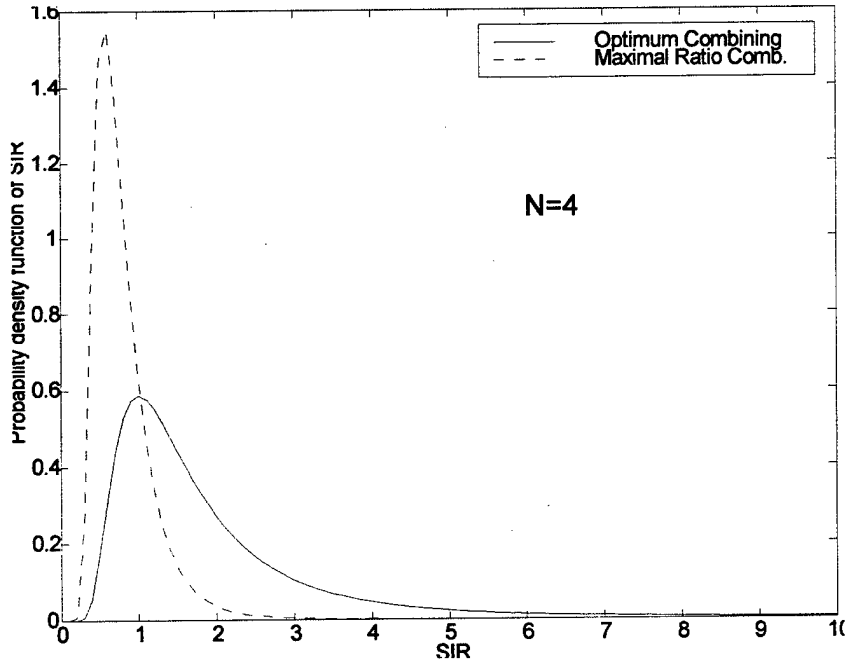

Figure 4.8: Density function of the frame SIR for $L = 6$ interference sources, non-fading/Rayleigh case.

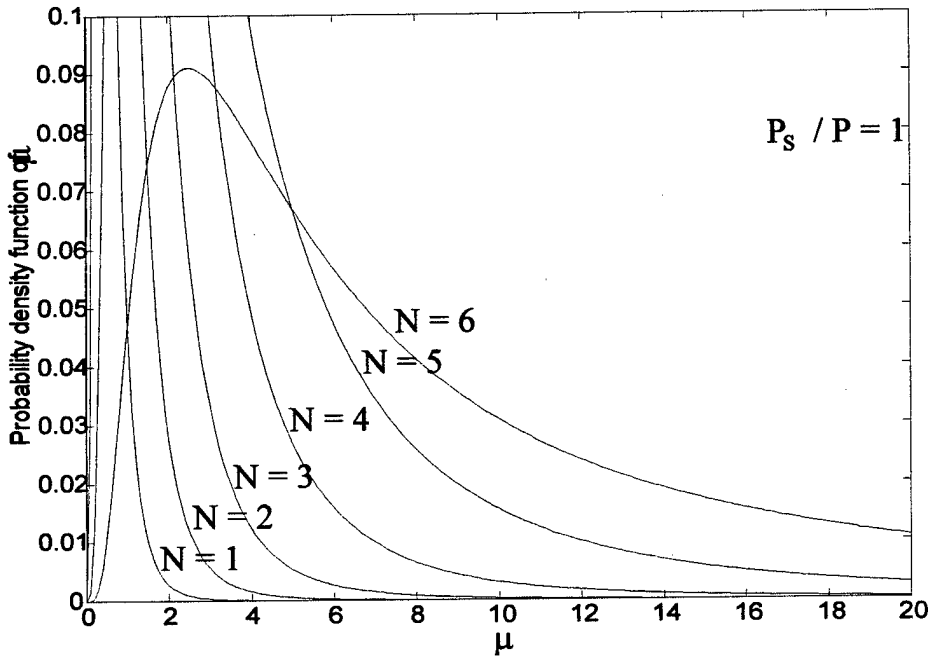

Figure 4.9: The effect of the number of antenna elements on the probability density function of μ

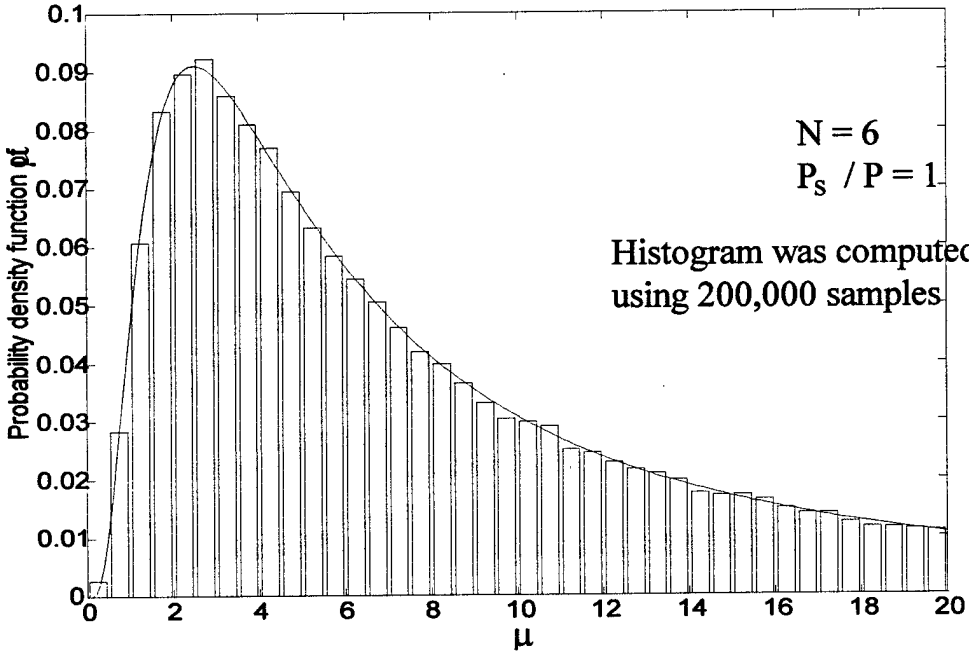

Figure 4.10: A comparison of the probability density function using theory and simulation

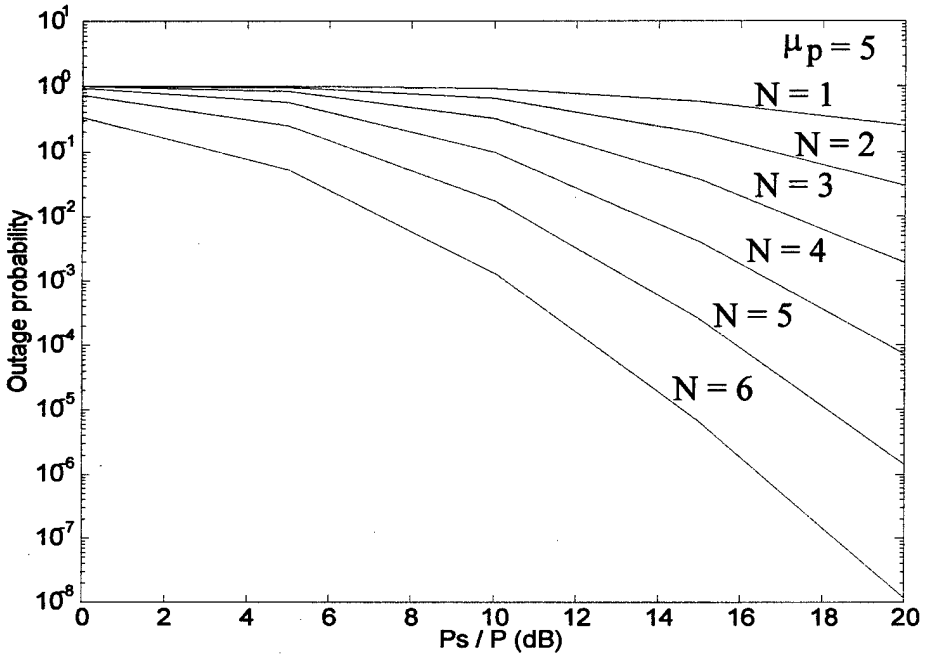

Figure 4.11: The outage probability versus $\frac{P_s}{P_I}$ with the number of antenna elements N at the parameter

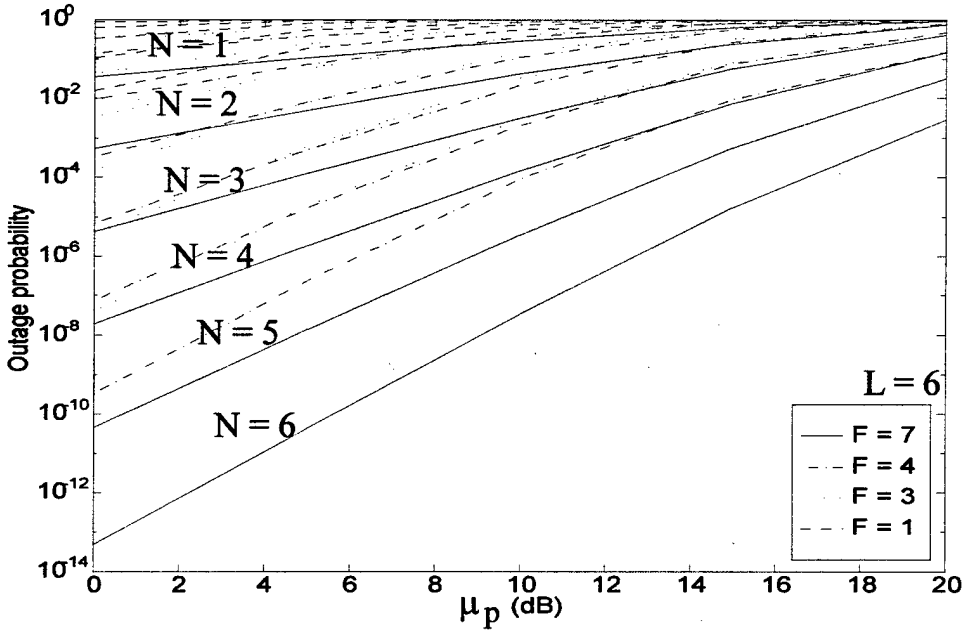

Figure 4.12: The average probability of bit error versus $\frac{P_s}{P_I}$ with the number of antenna elements N as the parameter

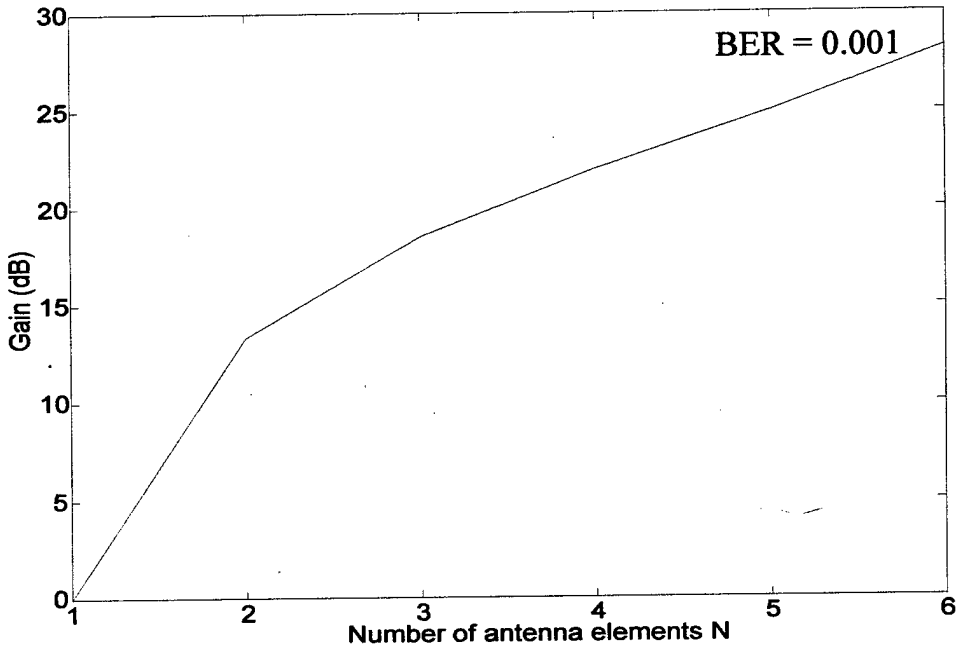

Figure 4.13: The diversity gain versus the number of antenna elements N

Chapter 5

Exact Bit Error Probability for Optimum Combining

In this chapter, we derive expressions for the *exact* bit error probability (BEP) for the detection of coherent binary PSK signals of the optimum combiner employing space diversity when both the desired signal and a Gaussian co-channel interferer are subject to flat Rayleigh fading. Two different methods are employed to reach two different, but numerically identical, expressions.

The first method is a direct approach of obtaining the conditional BEP and then averaging over fading of the SOI and CCI. The second method is based on the moment generating function (MGF) - based method [56]. The latter results in expressions that are easier to compute than the direct method. The same upper bound can be derived for each of the two method. Using methods delineated in this letter and in [56], results obtained by the MGF method can be easily extended to M-PSK and QAM modulations.

5.1 Moment Generating Function

Consider the reverse link (mobile to base) of a digital mobile radio communication system employing an N-element antenna array at the base station. The channel is assumed quasi-static, i.e., fixed over some arbitrary time of interest defined as a frame. The channel assumes uncorrelated realizations in different frames. Following carrier demodulation, matched filtering and sampling at the symbol interval, we change Expression (3.1) into:

$$\mathbf{u}(k) = \sqrt{P_1}a(k)\,\mathbf{c}_s + \mathbf{z}(k), \tag{5.1}$$

where $a(k) \in \{-1, 1\}$ is a binary symbol, P_1 and $\mathbf{c}_s$ are respectively, the power and the channel propagation vector for the SOI. With independent Rayleigh fading at each antenna, the vector $\mathbf{c}_s$ has a complex-valued multivariate Gaussian distribution with $E[\mathbf{c}_s] = \mathbf{0}$ and $E\left[\mathbf{c}_s\mathbf{c}_s^H\right] = \mathbf{I}$, where the superscript H denotes transpose and complex conjugate. It is further assumed that the interference can be expressed as

$$\mathbf{z}(k) = b(k)\,\mathbf{c}_I + \mathbf{n}(k), \tag{5.2}$$

where the amplitude $b(k)$ has a zero-mean, complex-valued Gaussian distribution with variance P_2, $\mathbf{c}_I$ is the interference propagation vector which is i.i.d. with $\mathbf{c}_s$, and $\mathbf{n}(k)$ is zero-mean, white spatial noise with $E\left[\mathbf{n}(k)\mathbf{n}^H(k)\right] = \sigma^2\mathbf{I}$. With this signal model, the interference is Gaussian conditional on the vector $\mathbf{c}_I$. The interference spatial covariance matrix in effect over the period of a frame is given by $\mathbf{R} = E\left[\mathbf{z}(k)\mathbf{z}^H(k) \mid \mathbf{c}_I\right] = P_2\mathbf{c}_I\mathbf{c}_I^H + \sigma^2\mathbf{I}$.

The maximum SINR at the array output is given by

$$\mu = P_1\mathbf{c}_s^H\mathbf{R}^{-1}\mathbf{c}_s. \tag{5.3}$$

Note that the SINR μ is conditioned on $\mathbf{c}_s$ and $\mathbf{c}_I$, and thus it varies at the fading rate. Eq. (5.3) can be expressed as

$$\mu = P_1\mathbf{c}_s^H\mathbf{Q}\Lambda^{-1}\mathbf{Q}^H\mathbf{c}_s, \tag{5.4}$$

where Λ is a diagonal matrix of the eigenvalues $\{\lambda_1, \ldots, \lambda_N\}$ of $\mathbf{R}$ and $\mathbf{Q}$ is unitary matrix. Let $\mathbf{s} = \mathbf{Q}^H\mathbf{c}_s$. Since $\mathbf{Q}$ is unitary, the elements of $\mathbf{s}$ retain the properties of the elements of $\mathbf{c}_s$. Thus eq. (5.4) can be rewritten as

$$\mu = P_1\sum_{i=1}^{N}\frac{|s_i|^2}{\lambda_i}, \tag{5.5}$$

where $\mathbf{s}^T = [s_1, \ldots, s_N]$. Since the elements of $\mathbf{c}_s$ have complex-valued Gaussian distributions, each term $|s_i|^2$ is a chi-square random variable with two degrees of freedom. The eigenvalues $\{\lambda_i\}$ of $\mathbf{R}$ are

$$\lambda_i = \begin{cases} P_2\sum_{n=1}^{N} \mid c_{I,n} \mid^2 + \sigma^2 & \text{i=1} \\ \sigma^2 & i = 2, \ldots, N, \end{cases}$$

where $\mathbf{c}_I^T = [c_{I,1}, \ldots, c_{I,N}]$. Each of $\{\mid c_{I,n} \mid^2\}$ is a chi-square random variable with two degrees of freedom.

Due to the mutual independence of the terms in eq. (5.5), the moment generating function (MGF) of μ conditioned on λ_1 is given by [57]:

$$\phi_{\mu/\lambda_1}(s) = \frac{1}{\left(1 - s\frac{P_s}{\lambda_1}\right)\left(1 - s\frac{P_s}{\sigma^2}\right)^{N-1}}, \tag{5.6}$$

where $P_s = P_1\mathrm{E}\left[|c_{s,n}|^2\right], n = 1, \ldots, N$, is the mean signal power per antenna and $\mathbf{c}_s^T = [c_{1,n}, \ldots, c_{s,N}]$. The MGF given above provides the starting point for each of the two methods of analysis.

5.2 Direct Method

Let $h \triangleq P_s/\sigma^2$ denote the mean SNR per antenna (channel). Therefore, the conditional probability density function (PDF) of μ can now be obtained by applying the inverse Laplace transformation to (5.6) and is given by [57, p. 410]:

$$f_{\mu/\lambda_1}(\mu) = \frac{\lambda_1\mu^{N-1}e^{\frac{-\lambda_1\mu}{P_s}}{}_1F_1\left(N-1; N; \frac{(\lambda_1-\sigma^2)\mu}{P_s}\right)}{\sigma^2\Gamma(N)h^N}, \quad \mu \geq 0,\ \lambda_1 \geq \sigma^2,\ N \geq 1, \tag{5.7}$$

where ${}_1F_1(\cdot)$ is the confluent hypergeometric function and $\Gamma(\cdot)$ is the standard gamma function. Clearly, if the interference is fading, λ_1 is a random variable that assumes new values at the fading rate. Note that in references [22, 23], λ_1 in (5.7) was assumed constant, i.e., it was replaced by its mean value, $E[\lambda_1] = NP_I + \sigma^2$, where $P_I = P_2\, E[|c_{I,n}|^2]$, $n = 1, \ldots, N$. Conditioned on λ_1, the probability of bit error is computed from

$$\begin{aligned} P_{e/\lambda_1} &= \int_0^\infty Q(\sqrt{2\mu}) f_{\mu/\lambda_1}(\mu) d\mu \\ &= \frac{1}{2} - \frac{1}{2}\int_0^\infty \mathrm{erf}(\sqrt{\mu}) f_{\mu/\lambda_1}(\mu) d\mu, \end{aligned} \tag{5.8}$$

where $Q(x) \triangleq \frac{1}{2\pi}\int_x^\infty exp(-\frac{y^2}{2})dy$ is the Gaussian Q-function and erf$(\cdot)$ is the error function. Using the identity $\mathrm{erf}(\sqrt{\mu}) = \frac{2}{\sqrt{\pi}}\sqrt{\mu}\, e^{-\mu}{}_1F_1\left(1; \frac{3}{2}; \mu\right)$ [58], and relation [59, p. 224] in (5.8), we get

$$P_{e/\lambda_1} = \frac{1}{2} - \frac{\lambda_1 \Gamma(N+\frac{1}{2}) P_s^{N+\frac{1}{2}} F_2\left(N+\frac{1}{2}, 1, N-1; \frac{3}{2}, N; \frac{P_s}{\lambda_1+P_s}, \frac{\lambda_1-\sigma^2}{\lambda_1+P_s}\right)}{\sqrt{\pi}\sigma^2\Gamma(N)h^N(\lambda_1+P_s)^{N+\frac{1}{2}}}, \tag{5.9}$$

where $F_2(\cdot)$ is Appell's hypergeometric function defined in [60]. It can be shown that the series in (5.9) converges.

Since each of $\{|\, c_{I,n}\,|^2\}$ has a chi-square distribution, $\lambda_1 = P_2 \sum_{n=1}^N |\, c_{2,n}\,|^2 + \sigma^2$, has the PDF

$$f_{\lambda_1}(\lambda_1) = \Gamma^{-1}(N) P_I^{-N} (\lambda_1 - \sigma^2)^{N-1} e^{-\frac{(\lambda_1-\sigma^2)}{P_I}},\ \lambda_1 \geq \sigma^2. \tag{5.10}$$

The BEP averaged over all values of λ_1 is given by

$$P_e = \int_0^\infty P_{e/\lambda_1} f_{\lambda_1}(\lambda_1) d\lambda_1. \tag{5.11}$$

Substituting (5.9) and (5.10) into (5.11),

$$\begin{aligned} P_e &= \frac{1}{2} - \frac{\Gamma(N+\frac{1}{2})P_s^{N+\frac{1}{2}}}{\sqrt{\pi}\sigma^2\Gamma(N)h^N} \frac{1}{\Gamma(N)P_I^N} \int_{\sigma^2}^\infty \frac{\lambda_1}{(\lambda_1+P_s)^{N+\frac{1}{2}}} (\lambda_1-\sigma^2)^{N-1} e^{-\frac{(\lambda_1-\sigma^2)}{P_I}} \\ &\quad \times F_2\left(N+\frac{1}{2}, 1, N-1; \frac{3}{2}, N; \frac{P_s}{\lambda_1+P_s}, \frac{\lambda_1-\sigma^2}{\lambda_1+P_s}\right) d\lambda_1. \end{aligned} \tag{5.12}$$

A closed form expression for the integral in (5.12) is not known, however, the integral can be evaluated numerically.

A simpler upper bound can be derived for (5.12). Using the bound $Q(\sqrt{2\mu}) \leq \frac{1}{2}e^{-\mu}$ and integral tables [59, p. 223] in eq. (5.8), we get

$$P_{e/\lambda_1} \leq \frac{1}{2} \frac{\lambda_1}{(\lambda_1+P_s)(1+h)^{N-1}}. \tag{5.13}$$

The expression in (5.13) provides meaningful insight into a few special cases. When there is no interference, i.e., $P_2 = 0, \lambda_1 = \sigma^2$, the conditional BEP of (5.13) reduces to $P_e \leq$

$\frac{1}{2}(1+h)^{-N}$. This is the upper bound for the BEP of an N-order space diversity receiver employing maximal ratio combining (MRC), as expected. When the interference power is large, i.e., $P_2 \to \infty$, ($\lambda_1 \to \infty$), (5.13) reduces to $P_e \leq \frac{1}{2}(1+h)^{-(N-1)}$. This is the upper bound for the BEP of an $(N-1)$-order diversity MRC receiver without interference. Thus the presence of an interference with infinite power results in the loss of one diversity path, a result first mentioned in [22, 23].

5.3 Moment Generating Function Method

This part was contributed by Alouini and Simon.

In this section, the MGF-based method is used to develop the exact BEP for BPSK modulation with optimum combining in the presence of a Gaussian CCI when both SOI and CCI are subject to Rayleigh fading.

Using the alternate representation of the Gaussian Q-function [56], namely,

$$Q(x) = \frac{1}{\pi}\int_0^{\pi/2} \exp\left(-\frac{x^2}{2\sin^2\theta}\right) dx, \tag{5.14}$$

and after reversing the order of integration, eq. (5.8) can be rewritten as

$$P_{e|\lambda_1} = \frac{1}{\pi}\int_0^{\pi/2}\int_o^{\infty} \exp\left(-\frac{\mu}{\sin^2\theta}\right) f_{\mu|\lambda_1}(\mu) d\mu dx \tag{5.15}$$

$$= \frac{1}{\pi}\int_0^{\pi/2} \phi_{\mu|\lambda_1}\left(-\frac{1}{\sin^2\theta}\right) d\theta, \tag{5.16}$$

where the MGF $\phi_{\mu|\lambda_1}(s)$ conditional on λ_1 is given by (5.6). Now averaging the conditional BEP of (5.15) combined with (5.6) over the PDF of λ_1 given by (5.10), we obtain

$$P_e = \frac{1}{\pi\Gamma(N)P_I^N}\int_0^{\pi/2} \frac{1}{\left(1+\frac{1}{\sin^2\theta}h\right)^{N-1}} \int_{\sigma^2}^{\infty} \frac{1}{\left(1+\frac{1}{\sin^2\theta}\frac{P_s}{\lambda_1}\right)} (\lambda_1-\sigma^2)^{N-1} \exp\left(-\frac{\lambda_1-\sigma^2}{P_I}\right) d\lambda_1 d\theta. \tag{5.17}$$

Now letting $y = (\lambda_1 - \sigma^2)/P_I$, and recognizing that

$$\frac{\sigma^2}{P_I} = \frac{P_s}{hP_I}, \tag{5.18}$$

then, (5.17) becomes

$$P_e = \frac{1}{\pi\Gamma(N)}\int_0^{\pi/2} \frac{1}{\left(1+\frac{1}{\sin^2\theta}h\right)^{N-1}} \int_0^{\infty} \frac{1+\frac{hP_I}{P_s}y}{\left(1+\frac{h}{\sin^2\theta}+\frac{hP_I}{P_s}y\right)} y^{N-1}e^{-y} dy d\theta. \tag{5.19}$$

Finally, letting $z = \frac{hP_I}{P_s}y$, (5.19) becomes

$$P_e = \frac{1}{\pi\Gamma(N)}(\frac{P_s}{hP_I})^N \int_0^{\pi/2} \frac{1}{\left(1+\frac{1}{\sin^2\theta}h\right)^{N-1}} \int_0^{\infty} \frac{1+z}{\left(1+\frac{h}{\sin^2\theta}+z\right)} z^{N-1} \exp\left(-\frac{P_s}{hP_I}z\right)\, dzd\theta. \tag{5.20}$$

To evaluate the integral on z, we use [61, p.336, eq.(3.383.10)]. We have,

$$\int_0^{\infty} \frac{1+z}{\beta+z} z^{v-1}e^{-\mu z}dz = \beta^{v-1}e^{\beta\mu}\Gamma(v)\Gamma(1-v,\beta\mu) + \beta^v e^{\beta\mu}\Gamma(v+1)\Gamma(-v,\beta\mu), \tag{5.21}$$

where $\Gamma(a,x)$ is the complementary incomplete gamma function [61, p.950]. Recognizing from (5.21) that $\beta = 1+\frac{h}{\sin^2\theta}$, $v = N$ and also that $\Gamma(N+1)/\Gamma(N) = N$, we obtain after some simplification the final desired result

$$\begin{aligned} P_e &= \frac{1}{\pi}(\frac{P_s}{hP_I})^N \int_0^{\pi/2} \exp\left\{\left(1+\frac{h}{\sin^2\theta}\right)\frac{P_s}{hP_I}\right\} [\Gamma\left(1-N, \left(1+\frac{h}{\sin^2\theta}\right)\frac{P_s}{hP_I}\right) \\ &\quad +N\left(1+\frac{h}{\sin^2\theta}\right)\Gamma\left(-N, \left(1+\frac{h}{\sin^2\theta}\right)\frac{P_s}{hP_I}\right)]d\theta, \end{aligned} \tag{5.22}$$

If one wants to simplify the notation a bit, then define

$$f(\theta) \triangleq \left(1+\frac{h}{\sin^2\theta}\right)\frac{P_s}{hP_I}, \tag{5.23}$$

in which case (5.22) simplifies to

$$P_e = \frac{1}{\pi}\left(\frac{P_s}{hP_I}\right)^N \int_0^{\pi/2} e^{f(\theta)}\left[\Gamma\left(1-N, f(\theta)\right) + N\frac{hP_I}{P_s}f(\theta)\Gamma(-N, f(\theta))\right] d\theta. \tag{5.24}$$

This is an exact result which involves a single integral with finite limits and an integrand composed of an exponential and two complementary incomplete gamma functions. This should be compared with the BEP obtained via the direct method in (5.12), which involves a semi-infinite integral with an integrand containing the more complicated Appell hypergeometric function (not readily found in standard software packages such as Mathematica). It is of interest to examine the special cases with the MGF method.

For the special case of no interferer, i.e., $P_I = 0$, ($\lambda_1 = \sigma^2$), eq. (5.19) becomes

$$P_e = \frac{1}{\pi\Gamma(N)} \int_0^{\pi/2} \frac{1}{\left(1+\frac{h}{\sin^2\theta}\right)^N} \int_0^{\infty} y^{N-1}e^{-y}dyd\theta. \tag{5.25}$$

Using [61, eq.(3.381.4)], eq. (5.25) simplifies to

$$P_e = \frac{1}{\pi}\int_0^{\pi/2} \frac{1}{\left(1+\frac{h}{\sin^2\theta}\right)^N} d\theta, \tag{5.26}$$

which corresponds to the performance of coherent PSK with MRC and an N-element array.

For the special case of a single infinite power interferer, i.e., $P_I = \infty$ ($\lambda_1 = \infty$), eq. (5.25) simplifies to

$$\begin{aligned} P_e &= \frac{1}{\pi\Gamma(N)}\int_0^{\pi/2} \frac{1}{\left(1+\frac{h}{\sin^2\theta}\right)^{N-1}} \int_0^{\infty} y^{N-1}e^{-y}dyd\theta \\ &= \frac{1}{\pi}\int_0^{\pi/2} \frac{1}{\left(1+\frac{h}{\sin^2\theta}\right)^{N-1}} d\theta. \end{aligned} \tag{5.27}$$

Thus, based on *exact* expressions for BEP, we observe that for the infinite power interferer, the array uses up one entire order of diversity to cancel it. This same conclusion was reached via the direct method only based on the upper bound (5.13) on conditional BEP and in [23] based on approximate expressions for average BEP (obtained by replacing λ_1 by $E[\lambda_1] = NP_I + \sigma^2$).

5.3.1 Bounds on Average BEP

Strict upper bounds on the conditional BEP are easily obtained from (5.15) combined with (5.6). In particular, the conditional BEP is given by

$$P_{e|\lambda_1} = \frac{1}{\pi}\int_0^{\pi/2} \frac{1}{\left(1+\frac{1}{\sin^2\theta}h\right)^{N-1}} \frac{1}{\left(1+\frac{1}{\sin^2\theta}\frac{P_s}{\lambda_1}\right)} d\theta. \tag{5.28}$$

Since the integrand is maximum at the upper limit, i.e., $\theta = \pi/2$, then upper bounding the integrand by its value at $\theta = \pi/2$ gives the upper bound on the conditional BEP as

$$P_{e|\lambda_1} \leq \frac{1}{2}\frac{\lambda_1}{(\lambda_1 + P_s)}\frac{1}{(1+h)^{N-1}}. \tag{5.29}$$

This is the same result as (5.13). The bound on the average P_e is then obtained after some manipulations by averaging the left-hand side of the previous expression over the density function of λ_1 in (5.10):

$$P_e \leq A\left[(N-1)! - (-1)^{N-2}\frac{P_s}{P_I}\eta^{N-1}e^{\eta}\,\mathrm{Ei}(-\eta) + \sum_{k=1}^{N-1}(k-1)!\,(-\eta)^{N-1-k}\right] \tag{5.30}$$

where $\mathrm{Ei}(\cdot)$ is the exponential integral, $A = \left(2(1+h)^N\Gamma(N)\right)^{-1}$ and $\eta = (P_s + \sigma^2)/P_I$.

5.4 Numerical Results

Numerical results are provided to illustrate the analysis presented in the letter. Results are shown for binary PSK modulation. Relations (5.12) and (5.24) provide the exact BEP via the direct and MGF methods, respectively. Numerical evaluation of the two relations shows that they are indistinguishable as they should be since they are both exact. In Figure 5.1, eq. (5.12)/(5.24) and [[23, p. 223], eq. (25)] are plotted as a function of average total SNR defined as $N\frac{P_s}{\sigma^2}$, where N is the order of diversity. The difference between the curves obtained using eq. (5.12) and [[23, p. 223], eq. (25)] is small, but evident. This difference is more evident in Figure 5.2, which zooms in on part of Figure 5.1. There is a simple explanation as to why the values of the probabilities that we obtained are numerically close to those in [[23, p. 223]]. The performance, i.e., the BEP, of the optimum combiner is shown for the cases $N = 2,\ 4$. In either case, the array has sufficient number of degrees of freedom to suppress the interference, regardless of whether the interference is fading or non-fading.

5.5 Discussion

In this chapter, we developed expressions (eqs. (5.12),(5.24)) for the exact BEP of the optimum combiner of BPSK signals with Gaussian co-channel interference in flat Rayleigh fading. Unlike previous work, this expression takes into account the density function of the fading interference. The closeness of the exact expression to the approximation using the average interference power justifies the use of the approximation in practice.

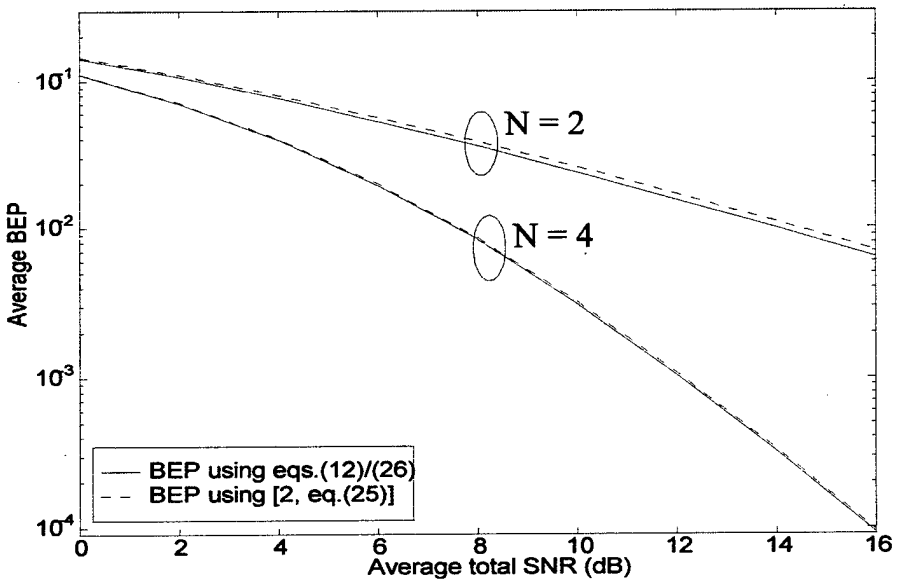

Figure 5.1: BEP of the optimum combiner in Rayleigh fading with a fading Gaussian co-channel interferer.

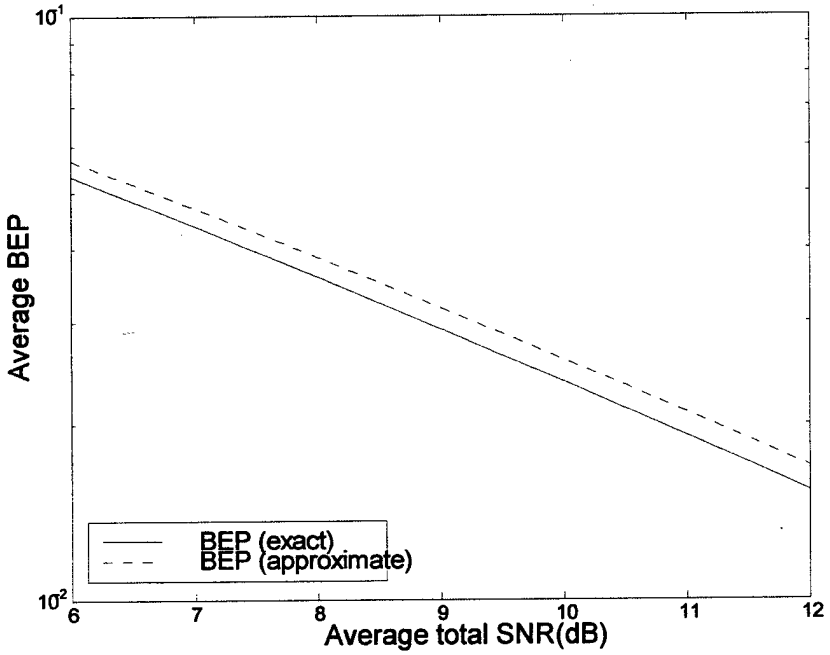

Figure 5.2: BEP performance on a magnified scale, $N = 2$ antennas.

Chapter 6

Analysis of CDMA system with MRC

This chapter is attempted to provide a comprehensive analysis which joins several of the most important factors affecting the performance of CDMA systems. In particular, new analytical expressions are developed for the outage and bit error probability (BEP) of CDMA systems. These expressions account for adverse effects such as path loss, large-scale fading (shadowing), small-scale fading (Rayleigh fading), and CCI, as well as for correcting mechanisms such as power control (compensates for path loss and shadowing), spatial diversity (mitigates against Rayleigh fading), and voice activity gating (reduces CCI). The new expressions may be used as convenient analysis tools that complement computer simulations. Of particular interest are trade-offs revealed among system parameters such as maximum allowed power control error versus the number of antennas used for spatial diversity.

6.1 Instantaneous Output SIR

Based on the signal model in Chapter 2.2, following spread spectrum demodulation and sampling at the symbol interval, the received signal can be written:

$$\begin{aligned} \mathbf{y}(i) &= \int_{iT_s}^{(i+1)T_s} \mathbf{x}(t)u_1(t)dt \\ &= \sqrt{\lambda_1}s_1(i)\mathbf{c}_1 + \sum_{k=2}^{K_u} \epsilon_k \sqrt{\lambda_k} \left(s_k(i-1)\rho_k^- + s_k(i)\rho_k^+ \right) \mathbf{c}_k, \end{aligned} \tag{6.1}$$

where $\rho_k^- = \int_{iT_s}^{iT_s+\tau_k} u_k(t-\tau_k)u_1(t)dt$, $\rho_k^+ = \int_{iT_s+\tau_k}^{(i+1)T_s} u_k(t-\tau_k)u_1(t)dt$ are the correlations between user signatures. It is assumed that the correlations above are independent of the symbol interval index i.

If the CCI is spatially white, the optimum output SIR is provided by maximal ratio combining (MRC). The array weight vector $\mathbf{w}$ then acts as a channel matched filter, $\mathbf{w} = \mathbf{c}_1$. The array output is expressed:

$$\begin{aligned} z(i) &= \mathbf{w}^H\mathbf{y}(i) = \mathbf{c}_1^H\mathbf{y}(i) \\ &= \phi_s(i) + \phi_j(i), \end{aligned} \tag{6.2}$$

where

$$\phi_s(i) = \sqrt{\lambda_1} s_1(i) \mathbf{c}_1^H \mathbf{c}_1 \tag{6.3}$$

and

$$\phi_j(i) = \mathbf{c}_1^H \sum_{k=2}^{K_u} \epsilon_k \sqrt{\lambda_k} \left(s_k (i-1) \rho_k^- + s_k (i) \rho_k^+ \right) \mathbf{c}_k \tag{6.4}$$

are the desired signal and CCI respectively, at the array output. Over the duration of a bit, it is assumed that the interference can be approximated by an equivalent source using the following expression:

$$\phi_j(i) = s(i) \mathbf{c}_1^H \sum_{k=2}^{K_u} \epsilon_k \sqrt{\eta_k \lambda_k} \mathbf{c}_k, \tag{6.5}$$

where $s(i)$ combines the total interference bit effects during the bit duration and η_k is a gain factor incorporating the effect of cross-correlation with the desired user's signal. This model is a worst case of sorts, in which interference sources are not independent, however, it has the advantage of being analytically tractable (see also [12]). The instantaneous output SIR is then written:

$$\gamma = \frac{|\phi_s(i)|^2}{|\phi_j(i)|^2}. \tag{6.6}$$

6.2 Computation of Outage Probability

The outage probability provides an indicator of how often the communication link's quality is under a specified acceptable level. The system capacity is generally computed for a prescribed outage level. The outage with respect to the *instantaneous* SIR was studied in [6]. In some case (for example, when the mobiles transmit voice rather than data), it is more suitable to consider the outage based on the *average* SIR (the averaging is over the Rayleigh fading).

Let the outage be defined as the probability that the average output SIR, γ_E, falls below a prescribed threshold γ_{th}, $P_{oE} = \Pr(\gamma_E < \gamma_{th})$, where the *average* SIR γ_E is given by:

$$\gamma_E = E\left[\frac{|\phi_s(i)|^2}{|\phi_j(i)|^2} \right]. \tag{6.7}$$

For maximal-ratio combining, the average output SIR :

$$\gamma_E = \sum_{m=1}^{M} \mu_m, \tag{6.8}$$

where μ_m is the single element input SIR. In our system model, the input SIR is assumed to be equal at all elements, $\mu_m = \mu$, then $\gamma_E = M\ \mu$, where μ is defined by:

$$\mu = \frac{\lambda}{\mathcal{J}} = \frac{\lambda}{\sum_{k=2}^{K_u} \epsilon_k \eta_k \lambda_k}. \tag{6.9}$$

It is noted that the *average* SIR is conditioned on the realization of μ. For full characterization of γ_E, it is necessary to determine the density of μ. Since $\epsilon_k \in \{0,1\}$, $\mathcal{J}$ is the sum of log-normal random variables. The number of elements in the sum is $\sum_{k=2}^{K_u} \epsilon_k$. Following Wilkinson's method [62, 24], $\mathcal{J}$ is approximated by a log-normal random variable; it is then proceeded to match $E[\mathcal{J}]$ and $E[\mathcal{J}^2]$ with the corresponding cumulants of the log-normal distribution. In [6], expressions are found for the mean m_g and variance σ_g of the normal variate $g = \ln \mu$. It follows that the outage probability can be written:

$$P_{oE} = \Pr\left(g < \ln \frac{\gamma_{th}}{M}\right). \tag{6.10}$$

Since g is normally distributed, (6.10) can be expressed

$$P_{oE} = 1 - Q\left(\frac{\ln \frac{\gamma_{th}}{M} - m_g}{\sigma_g}\right), \tag{6.11}$$

where $Q(x) = \int_x^\infty \frac{1}{\sqrt{2\pi}} e^{-x^2/2} dx$ is the Gaussian tail function.

Relation (6.11) provides the closed-form computation of the *average* SIR outage probability as a function of Rayleigh fading, PCE, and voice activity. When the communication link's quality is sensitive to the *instantaneous* SIR, the result in [6] should be used to evaluate the outage probability.

6.3 Computation of the Probability of Bit Error

Computation of the bit error requires knowledge of the distribution of the interference at array output. Due to dissimilar shadowing and fading affecting the various users, interferers are not identically distributed, hence the central limit theorem cannot be strictly invoked to claim the Gaussian property. Nevertheless, the Gaussian property is often assumed in such analyses [30, 33, 63, 64]. In this paper, the Gaussian assumption is validated by a chi-square test presented in the next section.

For BPSK and Gaussian interference, the conditional BEP is given by

$$b = P(e \mid \gamma) = Q\left(\sqrt{2\gamma}\right), \tag{6.12}$$

where γ is the *instantaneous* SIR and is given by:

$$\gamma = \frac{\lambda_1 \left|\mathbf{c}_1^H \mathbf{c}_1\right|^2}{\left|\mathbf{c}_1^H \sum_{k=2}^{K_u} \epsilon_k \sqrt{\eta_k \lambda_k}\, \mathbf{c}_k\right|^2}. \tag{6.13}$$

The variate γ is a function of Rayleigh fading, shadowing (PCE), and voice activity. The distribution of γ is required to determine the average probability of bit error. The conditional density of γ was found in [11, 12]

$$f_\gamma(\gamma \mid \mu) = \frac{M(\gamma/\mu)^{M-1}}{\mu(1+\gamma/\mu)^{M+1}}. \tag{6.14}$$

where μ was defined in (6.9). The BEP b is a function of the instantaneous SIR γ, hence a random variable. The density of b can be found from [65, p.125]:

$$f_b(b \mid \mu) = \left.\frac{f_\gamma(\gamma \mid \mu)}{|db/d\gamma|}\right|_{\gamma=\frac{1}{2}[Q^{-1}(b)]^2}, \tag{6.15}$$

where Q^{-1} is the inverse function of Q. After a few manipulations it can be shown that,

$$\frac{db}{d\gamma} = -\frac{1}{2\sqrt{\gamma\pi}}\, e^{-\gamma}. \tag{6.16}$$

Substituting (6.16) into (6.15), one has the conditional density of b,

$$f_b(b \mid \mu) = \left.\frac{M\,(\gamma/\mu)^{M-1}}{\mu\,(1+\gamma/\mu)^{M+1}}\; 2\sqrt{\gamma\pi}\; e^{\gamma}\right|_{\gamma=\frac{1}{2}[Q^{-1}(b)]^2}. \tag{6.17}$$

The function Q^{-1} can be evaluated by numerical integration. The unconditional density of b can be obtained by averaging over the distribution of μ

$$f_b\,(b) = \int_0^\infty f_b\,(b \mid \mu)\;\; f_\mu\,(\mu)\, d\mu. \tag{6.18}$$

Replacing μ by $\mu = e^g$, one gets

$$\begin{aligned} f_b\,(b) &= \int_0^\infty f_b\,(b \mid e^g)\;\; f_g\,(g)\;\; e^g\; dg \\ &= E_g\,[G\,(b,g)]\,, \end{aligned} \tag{6.19}$$

where $f_g\,(g) = f_\mu\,(g)\,/\,|dg/d\mu|_{\mu=e^g}$ and $G\,(b,g) = f_b\,(b \mid e^g)\;\; e^g$. Since μ has a log-normal distribution, $g = \ln\mu$ is normally distributed. An exact closed-form result for the integral in (6.19) is not available, however an approximation exists for $E_g\,[G(b,g)]$ when g has a normal distribution. The approximation is valid for an arbitrary probability function $G(b,g)$ and is expressed in terms of the mean m_g and the standard deviation σ_g [66]:

$$f_b\,(b) \cong \frac{2}{3}G(b,\, m_g) + \frac{1}{6}G(b,\, m_g + \sqrt{3}\,\sigma_g) + \frac{1}{6}G(b,\, m_g - \sqrt{3}\,\sigma_g). \tag{6.20}$$

The computation of the mean and variance of g, m_g and σ_g, respectively, is discussed in [6], thus the previous relation expresses $f_b(b)$ in terms of known quantities. To reiterate, $f_b(b)$ accounts for the effects of Rayleigh fading, shadowing (PCE), and voice activity. The BEP density function in (6.20) is a more complete characterization of system performance than the more common average BEP. The latter, can be obtained by using the density of b, or from the following argument. The conditional BEP can be expressed as:

$$\begin{aligned} P(e \mid \mu) &= \int_0^\infty P(e \mid \gamma)\, f_\gamma(\gamma \mid \mu)\, d\gamma \\ &= M\mu \int_0^\infty Q\left(\sqrt{2\gamma}\right) \frac{\gamma^{M-1}}{(\mu+\gamma)^{M+1}} d\gamma. \end{aligned} \tag{6.21}$$

Following [46], (6.21) can be expressed utilizing hypergeometric functions:

$$\begin{aligned} P(e \mid \mu) &= \frac{M}{2\Gamma(M+1)} \left[2\mu\Gamma(M+1)\, {}_2F_2(M+1,1;3/2,2;\mu)\right. \\ &\quad \left. -2\sqrt{\mu}\,\Gamma(M+1/2)\, {}_2F_2(M+1/2,1/2;1/2,3/2;\,\mu) + \Gamma(M)\right], \end{aligned} \tag{6.22}$$

where ${}_2F_2(\cdot)$ is the standard generalized hypergeometric function [39]. Expression (6.22) can be evaluated numerically by using software packages such as Maple, Mathematica, etc. Alternatively, (6.21) can be evaluated numerically. The unconditional BEP is found by averaging $P(e \mid \mu)$ over the distribution of μ:

$$P_e = \int_0^\infty P(e \mid \mu)\, f_\mu(\mu)\, d\mu \tag{6.23}$$

In terms of the normal random variable g, $g = \ln \mu$, one gets

$$P_e = \int_{-\infty}^\infty P(e \mid g)\, f_g(g)\, dg = E_g\left[P(e \mid g)\right]. \tag{6.24}$$

Finally, using the same approach as in (6.20), one can obtain the average probability of bit error:

$$\begin{aligned} P_e &= E_g\left[P(e \mid g)\right] = E_g\left[H(g)\right] \\ &\cong \frac{2}{3} H(e^{m_g}) + \frac{1}{6} H\left(e^{m_g+\sqrt{3}\sigma_g}\right) + \frac{1}{6} H\left(e^{m_g-\sqrt{3}\sigma_g}\right), \end{aligned} \tag{6.25}$$

where we introduced $H(g) = P(e \mid g)$ as a notational convenience.

6.4 Extensions of Previous Results

Some of the results obtained previously can be extended to more general cases. These include: other cell interference, correlation of shadowing among users, channel with time dispersion, pilot tone effect, and performance analysis in terms of Erlang capacity. These effects are discussed below.

Other Cell Interference. CCI is caused by inter-cell interference as well as intra-cell interference. This is particularly true for CDMA, for which the reuse factor is one. The other cell interference was studied in [67, 68]. If the same traffic load is assumed in all cells, the effect of CCI introduced by users of all other cells is equivalent to the effect of CCI from qK_u users of the home cell, where q is a factor that is determined empirically. With $K'_u \triangleq K_u(1+q)$, all the results developed so far apply with K_u replaced by K'_u.

Correlation of Shadowing Among Users. The analysis of the outage probability assumed independent shadowing among users. In practice, when signals received from different users are shadowed by the same obstacles in the vicinity of the base station, the shadowing affecting the users may be correlated. This requires some modifications in the computation of the quantities m_g and σ_g used in determining the outage probability P_{oE}. In [6] it is shown that the normal variate g (ln of the input SIR at each antenna element), is expressed in terms of the first and second moments of the interference power $\mathcal{J}$, $E[\mathcal{J}]$ and $E[\mathcal{J}^2]$, respectively. The computation of $E[\mathcal{J}]$, as shown in [6], is not affected by the correlation assumption. However, in the presence of correlation, the computation of $E[\mathcal{J}^2]$ is different than it is presented in [6]. We proceed now with this computation. By assumption, the power of the kth user λ_k, has a log-normal distribution, hence $\alpha_k = \ln \lambda_k$, has a normal distribution with some mean m_α and some variance σ_α^2. The shadowing correlation coefficient is defined as

$$r_{kj} = \frac{E[(\alpha_k - m_\alpha)(\alpha_j - m_\alpha)]}{\sigma_\alpha^2}, \tag{6.26}$$

where α_k and α_j are assumed identically distributed. For simplicity, we assume $r_{kj} = r$ for $k \neq j$ and $k, j = 1, \cdots, K_u$. We have,

$$\begin{aligned} E[\mathcal{J}^2] &= E\left[\left(\sum_{k=2}^{K_u} \epsilon_k \eta_k e^{\alpha_k}\right)^2\right] \\ &= \sum_{k=2}^{K_u} \eta_k^2 E\left[\epsilon_k^2 e^{2\alpha_k}\right] + 2\sum_{k=2}^{K_u}\sum_{j=k+1}^{K_u} \eta_k \eta_j E\left[\epsilon_k e^{\alpha_k} \epsilon_j e^{\alpha_j}\right] \\ &= pe^{2m_\alpha + 2\sigma_\alpha^2} \sum_{k=2}^{K_u} \eta_k^2 + p^2 e^{2m_\alpha} e^{\sigma_\alpha^2(1+r)} \sum_{k=2}^{K_u}\sum_{j\neq k} \eta_k \eta_j \equiv e^{\xi_2}, \end{aligned} \tag{6.27}$$

where p is the voice activity factor defined earlier. Using terminology from [6], the interference mean is expressed $E[\mathcal{J}] = e^{\xi_1}$. Letting $\mathcal{J} = e^\beta$, and since $\mathcal{J}$ is log-normal (hence β is normal), we also have

$$E[\mathcal{J}] = E\left[e^\beta\right] = e^{m_\beta + \sigma_\beta^2/2} = e^{\xi_1}, \tag{6.28}$$

$$E[\mathcal{J}^2] = E\left[e^{2\beta}\right] = e^{2m_\beta + 2\sigma_\beta^2} = e^{\xi_2}. \tag{6.29}$$

Solving for m_β and σ_β^2, we obtain

$$m_\beta = 2\xi_1 - \frac{1}{2}\xi_2, \tag{6.30}$$

$$\sigma_\beta^2 = \xi_2 - 2\xi_1. \tag{6.31}$$

Now, from (4.23) and the log-normality of λ_1 and $\mathcal{J}$, it follows that $\mu = \lambda_1/\mathcal{J}$ is also log-normal. We have

$$g = \ln \mu = \ln \frac{\lambda_1}{\mathcal{J}} = \alpha_1 - \beta. \tag{6.32}$$

The density function of μ is determined from the mean and variance of g, which can be expressed in terms of known quantities:

$$m_g = m_\alpha - m_\beta, \tag{6.33}$$
$$\sigma_g^2 = \sigma_\alpha^2 + \sigma_\beta^2 - 2r_{\alpha\beta}\sigma_\alpha\sigma_\beta, \tag{6.34}$$

where $r_{\alpha\beta}$ is the correlation efficient between α_1 and β. Once m_g and σ_g^2 were obtained, the computation of P_{oE} can be completed as in the uncorrelated case using (6.11).

The results above can be extended to the general case when r_{kj} are not equal, and α_k have different mean values and variances (see [69, 24] for more details about the expression of e^{ξ_2} and calculation of $r_{\alpha\beta}$).

Frequency-Selective Channel. The reverse link channel is assumed frequency-selective with L resolvable paths. A Rake receiver is used to track and combine the paths. Following spread spectrum demodulation, the signal received at the antenna array from the lth path can be written as an M-dimensional vector:

$$\begin{aligned}\mathbf{y}_l(i) &= \sqrt{\lambda_{1l}}\, s_1(i)\mathbf{c}_{1l} + \sum_{\substack{n=1\\ n\neq l}}^{L} \sqrt{\lambda_{1n}} \left(s_1(i-1)\rho_{1ln}^- + s_1(i)\rho_{1ln}^+\right)\mathbf{c}_{1n} \\ &\quad + \sum_{k=2}^{K_u}\sum_{n=1}^{L} \epsilon_k \sqrt{\lambda_{kn}} \left(s_k(i-1)\rho_{kln}^- + s_k(i)\rho_{kln}^+\right)\mathbf{c}_{kn}, \quad l = 1, \cdots, L,\end{aligned} \tag{6.35}$$

where $k = 1, \ldots, K_u$ is the user index, $n = 1, \ldots, L$ is the path index, λ_{kn} are the received signal powers, $\mathbf{c}_{kn}$ are the channel vectors, $\rho_{kln}^- = \int_{iT_s}^{iT_s+\tau_{kn}} u_k(t-\tau_{kn})u_1(t-\tau_{1l})dt$, $\rho_{kln}^+ = \int_{iT_s+\tau_{kn}}^{(i+1)T_s} u_k(t-\tau_{kn})u_1(t-\tau_{1l})dt$, τ_{kl} and τ_{kn} are the delays. Assume that the cross-correlations are independent of the path l, i.e., $\rho_{kln}^{-/+} = \rho_{kn}^{-/+}$. The various terms in (6.35) represent the desired signal, self-interference, and CCI, respectively. In the following, it is assumed that the self-interference contribution is negligible in comparison with the CCI. Signal vectors associated with the different paths, $\mathbf{y}_l(i)$ $(l = 1, \cdots, L)$, are stacked to form an ML-dimensional vector, $\mathbf{y}(i)$, and grouped according to components related to the desired signal and CCI, yielding the expression (see [70] for details):

$$\mathbf{y}(i) = \sqrt{\lambda_1} s_1(i)\, \mathbf{c}_1 + \mathbf{j}(i), \tag{6.36}$$

where $\mathbf{y}(i) = \left[\mathbf{y}_1^T(i), \cdots, \mathbf{y}_L^T(i)\right]^T$, $\mathbf{c}_1 = \left[\mathbf{c}_{11}^T, \cdots, \mathbf{c}_{1L}^T\right]^T$. The first term in the relation above represents the desired signal, $\mathbf{j}(i)$ is the interference, the superscript "T" denotes transpose. With MRC in both space (antenna array) and time (Rake) domains, the output is equivalent to applying MRC to the stacked vector in (6.36). The MRC weight vector is then given by

$\mathbf{w} = \mathbf{c}_1$. Similar to the approach taken earlier, it is assumed that the interference can be expressed as an equivalent source:

$$\mathbf{j}(i) = s(i) \sum_{k=2}^{K_u} \sum_{n=1}^{L} \epsilon_k \sqrt{\eta_{kn} \lambda_{kn}}\, \mathbf{c}_{kn}, \tag{6.37}$$

where $s(i)$ is the CCI source bit, η_{kn} is a gain factor representing the cross-correlation between codes. The double sum over the scaled ML-dimensional Gaussian distributed vectors $\mathbf{c}_{kn}$ is equivalent to another Gaussian vector,

$$\sum_{k=2}^{K_u} \sum_{n=1}^{L} \epsilon_k \sqrt{\eta_{kn} \lambda_{kn}}\, \mathbf{c}_{kn} = \sqrt{\mathcal{J}}\, \mathbf{c}_p, \tag{6.38}$$

where

$$\begin{aligned} \mathcal{J} &= \sum_{k=2}^{K_u} \sum_{n=1}^{L} \epsilon_k \eta_{kn} \lambda_{kn} \\ &= \sum_{k=2}^{K_u} \epsilon_k \nu_k \lambda_k, \end{aligned} \tag{6.39}$$

and $\nu_k = \sum_{n=1}^{L} \eta_{kn}$. The expression in (6.39) is similar in form to (6.37), thus the evaluation of the outage probability can continue as in the flat channel case. The distribution of the output SIR is obtained from (6.14), by substituting M with ML, to account for the additional diversity paths provided by the frequency-selective channel:

$$f_\gamma(\gamma \mid \mu) = \frac{ML(\gamma/\mu)^{ML-1}}{\mu(1+\gamma/\mu)^{ML+1}}. \tag{6.40}$$

All other results in the section hold by substituting M with ML.

Pilot-Aided Coherent Detection. In this case, the reverse link is assumed with pilot-aided coherent detection and perfect channel estimation. The power-split ratio for the pilot is r_p. Subsequently, the fraction of the total transmitted power that is used for the information traffic is $1/(1+r_p)$. With this model, the instantaneous output SIR is given by $\gamma' = \kappa\gamma$, where $\kappa = 1/(1+r_p)$, and γ was given in (6.13). Therefore distribution of the output SIR γ' is given by:

$$f_{\gamma'}(\gamma' \mid \mu) = \frac{M(\gamma'/\kappa\mu)^{M-1}}{\kappa\mu(1+\gamma'/\kappa\mu)^{M+1}}, \tag{6.41}$$

and P_{oE} and P_e can be modified accordingly. In particular, the outage probability is given by

$$P_{oE} = 1 - Q\left(\frac{\ln \frac{\gamma_{th}}{\kappa M} - m_g}{\sigma_g}\right). \tag{6.42}$$

Performance in Terms of Erlang Capacity. For a communication system, capacity may be measured in terms of the number of users per cell, or in terms of offered traffic intensity in Erlangs. Wireless system can be modeled as having Poisson traffic arrival, exponentially distributed service time, finite number of servers, and no waiting room (expressed as an $M/M/N/N$ queue). The system capacity of FDMA or TDMA is obtained by analyzing the blocking probability of an $M/M/N/N$ queue. Since users in CDMA systems all share a common spectral frequency band, the blocking condition of a CDMA system could be defined in a different way from that of FDMA or TDMA [25]. The blocking condition in CDMA systems will be defined as the case when the average SIR at base station falls below a prescribed level. This is the same definition as the outage referred to earlier in this section. For a finite number of communication channels, Poisson distribution cannot strictly represent the number of active users per cell. Nevertheless, the approximation of Poisson distribution is often used in the analysis [25, 68, 71]. Then the distribution of the number of active users in the system is given by:

$$P[K_u = k] = \frac{\zeta^k}{k!}\, e^{-\zeta}, \quad k = 0, 1, 2, \cdots \tag{6.43}$$

where ζ is determined by both call arrival rate and service rate. The mean value and variance of K_u are given by $\zeta = E[K_u] = \mathrm{var}[K_u]$. For simplicity, we assume that the factors η_k, defined following (6.5), are equal, $\eta_k = \eta$. The first and second moment of the interference $\mathcal{J}$ are to be averaged over K_u. From (6.37), and with $\lambda_k = e^{\alpha_k}$, we have

$$\begin{aligned} E[\mathcal{J}] &= E_{K_u}\left\{ E_{\epsilon_k,\alpha_k}\left[\sum_{k=2}^{K_u} \epsilon_k \eta_k e^{\alpha_k} \right] \right\} \\ &= (\zeta - 1)\, p\eta\, e^{m_\alpha + \sigma_\alpha^2/2} \equiv e^{\xi_1}; \end{aligned} \tag{6.44}$$

and

$$\begin{aligned} E[\mathcal{J}^2] &= E_{K_u}\left\{ E_{\epsilon_k,\alpha_k}\left[\left(\sum_{k=2}^{K_u} \epsilon_k \eta_k e^{\alpha_k} \right)^2 \right] \right\} \\ &= (\zeta - 1)\, p\eta^2\, e^{2m_\alpha + 2\sigma_\alpha^2} \\ &\quad + (\zeta^2 - 2\zeta + 2)\, p^2 \eta^2 e^{2m_\alpha + \sigma_\alpha^2} \equiv e^{\xi_2}, \end{aligned} \tag{6.45}$$

Using these expressions we can proceed to compute the relation between outage P_{oE} and Erlang capacity (ζ). The parameter ζ is amended to $\zeta(1+q)$ for $K_u' = K_u(1+q)$, if taking into account the other cell interference.

6.5 Numerical Results

Results in this section are derived from computer simulations of a CDMA system employing BPSK modulation and BPSK spreading, with a voice activity factor of $p = 3/8$ and a spreading ratio of 85. The spreading ratio corresponds to an information data rate of 14.4 kb/s and a signal bandwidth of 1.23 MHz. Unless specified otherwise, the number of antenna

elements assumed in the simulations was $M = 4$. The channel was assumed flat and subject to Rayleigh fading and shadowing.

First, the validity of the Gaussian approximation for the CCI was evaluated for $K_u = 30$ users, and PCE = 1.5 dB. To that end, the histogram of the interference level was generated and compared to the theoretical Gaussian curve. This is shown in Figure 6.1. Additionally, a chi-square test following the method presented in [65] was applied to evaluate the goodness of the fit. The sample space was partitioned into 21 disjoint intervals corresponding to a test with 20 degrees of freedom. Standard chi-square test tables show that for 20 degrees of freedom, the threshold for a 1% significance level is 37.57. Calculated from the simulation and averaged over 200 Monte Carlo runs, the chi-square statistic D^2 was 22.14, which does not exceed the threshold. It is concluded that the Gaussian approximation is valid for the interference.

The outage probability with respect to the *average* SIR is plotted in Figure 6.2 as a function of the capacity (number of users/cell) with the PCE as a parameter. For two-antenna selective diversity at cell site, adequate reverse link performance ($P_e < 10^{-3}$) is achievable with an array input of SIR < 5 [26], which is equivalent to array output SIR $<$ 7.5. If we use the same array output SIR requirement for the receiver in Figure 3.1, then the outage threshold is set at $\gamma_{th} = 7.5$. The analytical curves in Figure 6.2 are computed from (6.11), and the simulation curves are based on one million samples. For an outage of 10^{-2}, the system capacity is approximately 90, 47 and 24 users/cell for PCE = 0, 1.5, and 2.5 dB, respectively. Consequently, for PCE = 1.5 to 2.5 dB, the system capacity degrades 48% to 73% compared to the case of perfect power control. The effect of space diversity on the outage probability for *average* SIR is shown in Figure 6.3. For an outage of $P_{oE} = 10^{-2}$, the system capacity is about 9 to 72 users/cell for $M = 1$ to 6, i.e., the average capacity increase for each additional degree of space diversity is about 13 users/cell. A clear illustration of the trade-offs between the effects of antenna arrays and PCE can be found in Figure 6.4. The figure shows the capacity (computed analytically for $P_{oE}(\gamma_E < 7.5) = 0.01$) as a function of PCE and the number of antenna elements. The figure shows that for capacity of 30 users/cell, a two-element receiver at the base station requires the PCE to be less than 1 dB, while an six-element receiver can relax this requirement to 2.8 dB. The figure can be used to find the system capacity for a given PCE and for different number of antenna elements. Clearly, these results however, do not take into account effects such as coding and interleaving. For example, when PCE = 2.5 dB, the system capacity increases from 10 users/cell to 38 users/cell for an increase in the number of antennas from $M = 2$ to 6.

Figures 6.5 and 6.6 depict the distribution of the probability of bit error (b) with various values of PCE and number of antennas. These PDF curves shift toward to lower value of b as PCE decreases and the number of antennas increases. Figure 6.7 displays the analytical results for the average probability of bit error as a function of the number of users per cell. The system parameters are same as in Figure 6.2. If the desired performance is $P_e = 10^{-3}$, capacity is respectively 55, 45 and 32 users/cell for PCE = 0, 1.5, and 2.5 dB. In a CDMA system with a PCE from 1.5 to 2.5 dB, the system capacity degrades from 18% to 42% compared to the case of perfect power control.

Finally, we examined some of the extensions discussed in the previous sections. Figure 6.8 shows curves of outage probability versus capacity for PCE = 1.5 dB, $M = 4$ antennas, $L = 4$ time diversity paths, and different values of the correlation coefficient (r). For r from 0.2

to 1, the system capacity degrades from 6% to 21% compared to the case of uncorrelated shadowing ($r = 0$). Erlang capacity is shown in Figure 6.9. The figure depicts curves of outage probability versus Erlang capacity, $\zeta(1+q)$, for $M = 4$ antennas, $L = 1$ resolvable path, $r = 0$, voice activity $p = 3/8$, and PCE = 0, 1.5, and 2.5 dB, respectively. This figure parallels the results of Figure 6.2.

6.6 Discussion

In this chapter, we studied the reverse link performance of cellular CDMA systems, with space-time processing, Rayleigh fading, shadowing, power control error and voice activity gating. The performance was analyzed in terms of outage probability for average output SIR, as well as average probability of bit error. Analytical results were obtained that provide simple, but accurate approximations that can be used to evaluate system performance. All parameters needed for the computations can be obtained from measured data. The analysis shows that space-time processing provided by cell site antenna arrays along with a Rake receiver, compensates for performance degradations due to PCE in cellular CDMA systems. Computer simulations provided a good match to the analytical expressions developed in the context. It is noticed that the exact system performance improvement due to adaptive antenna arrays varies with the fading environment and cell layout. Since the implementation of adaptive antenna arrays introduces more digital signal processing and larger time delays, the interaction among the adaptive antenna, coding, interleaver, call processing and etc. requires further evaluation via simulations and field tests.

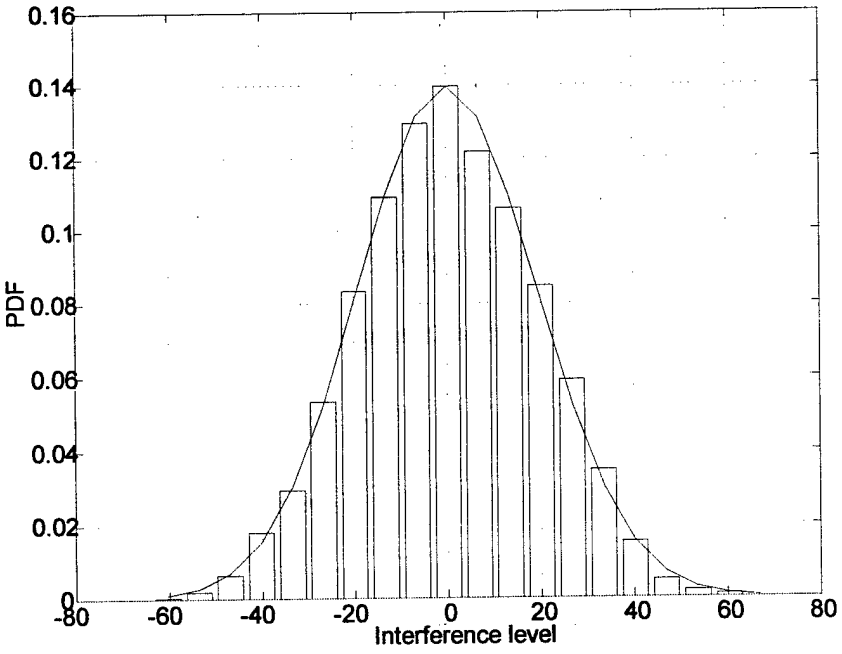

Figure 6.1: Gaussian fit to the interference histogram.

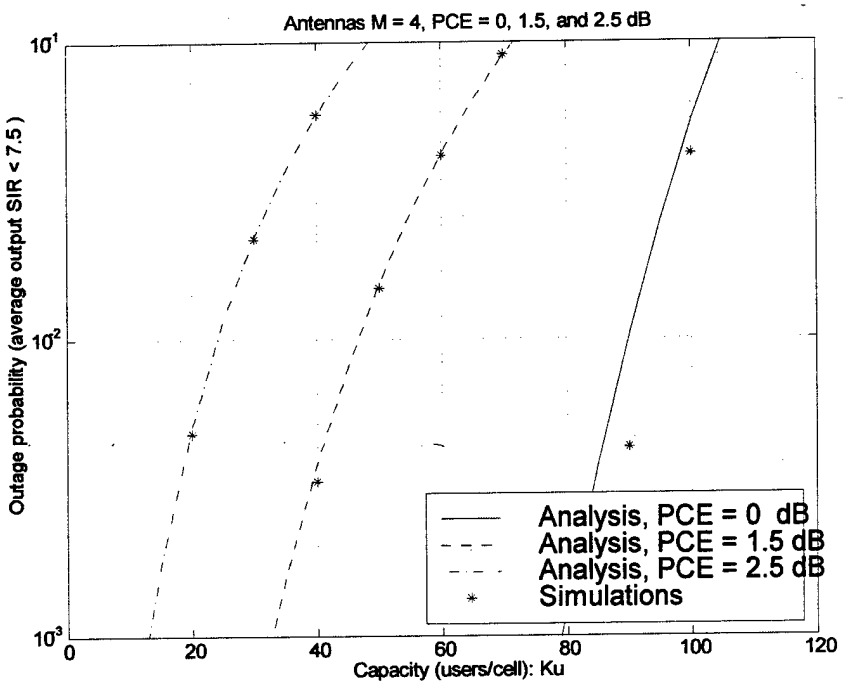

Figure 6.2: Outage probability versus capacity (users/cell), based on *average* SIR, for four antenna elements $M = 4$, various PCE's, and $p = 3/8$.

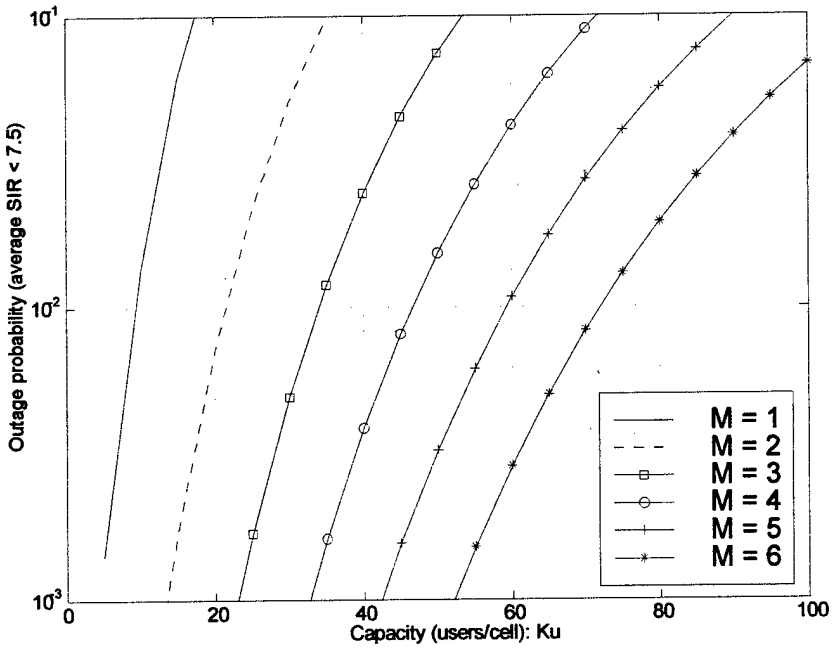

Figure 6.3: Outage probability versus capacity (users/cell), based on *average* SIR. Analytical results for PCE = 1.5 dB, $M = 1$ to 6, and $p = 3/8$.

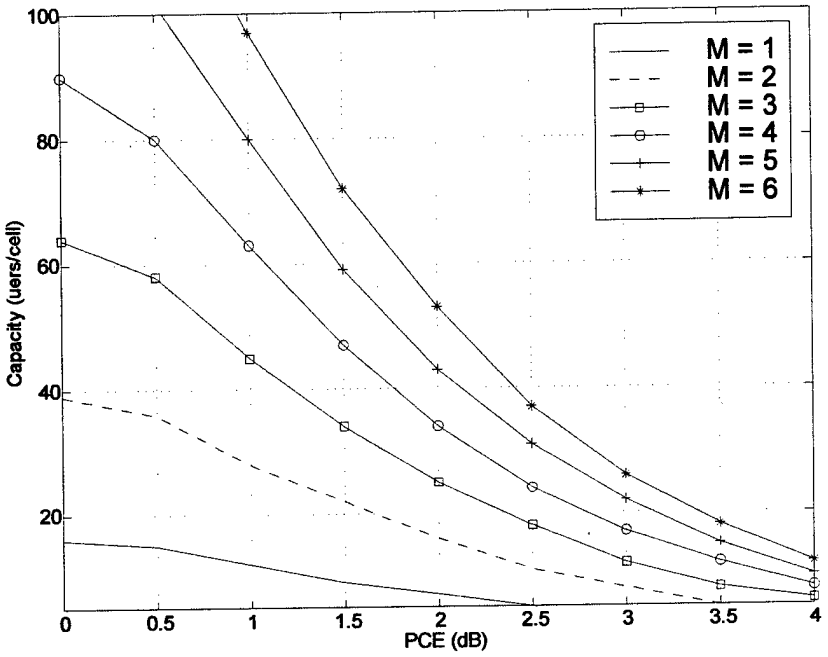

Figure 6.4: Capacity (users/cell) versus PCE for P_{oE} $(\gamma_E < 7.5) = 0.01$. Analytical results for $M = 1$ to 6, and $p = 3/8$.

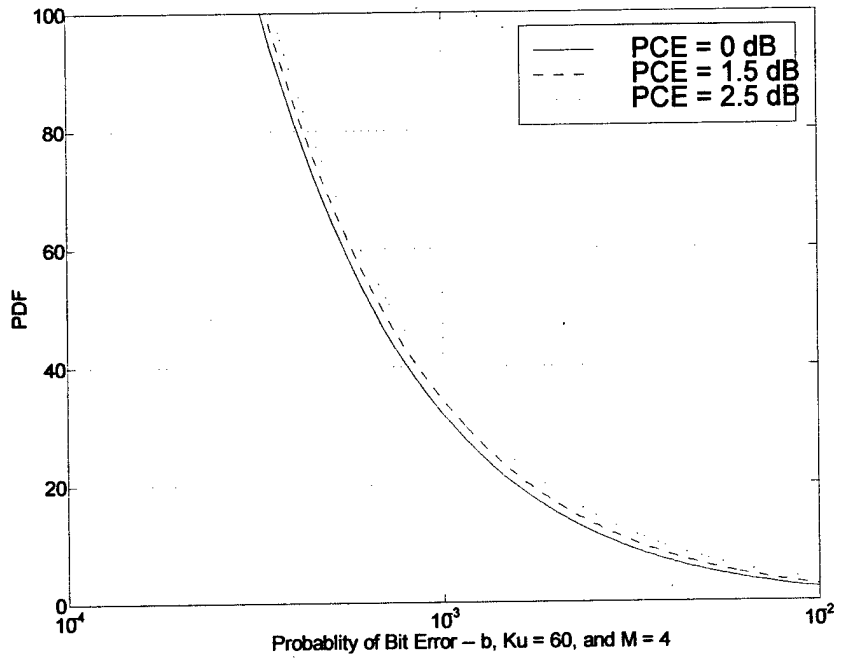

Figure 6.5: PDF of probability of bit error with $K_u = 100$ and $M = 4$.

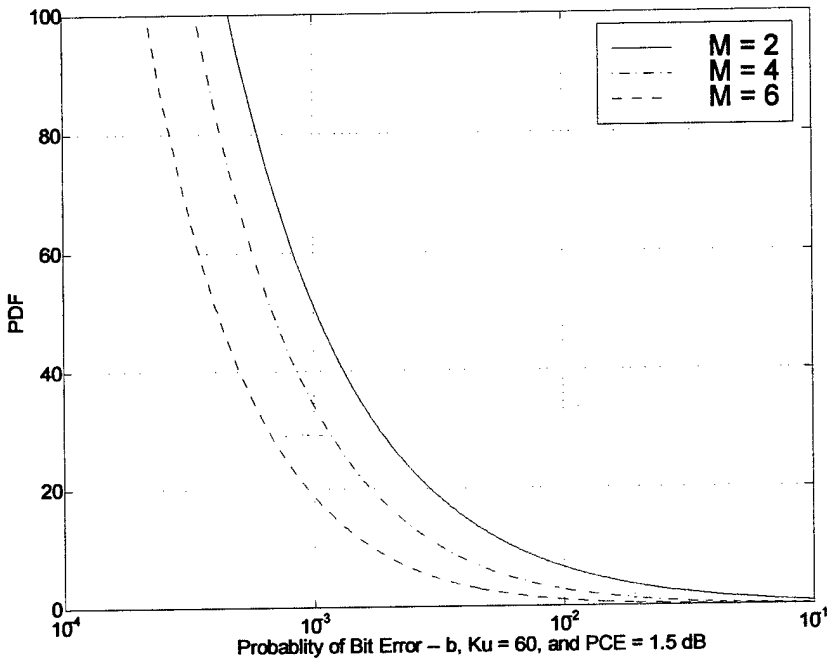

Figure 6.6: PDF of probability of bit error with $K_u = 100$ and PCE = 1.5 dB.

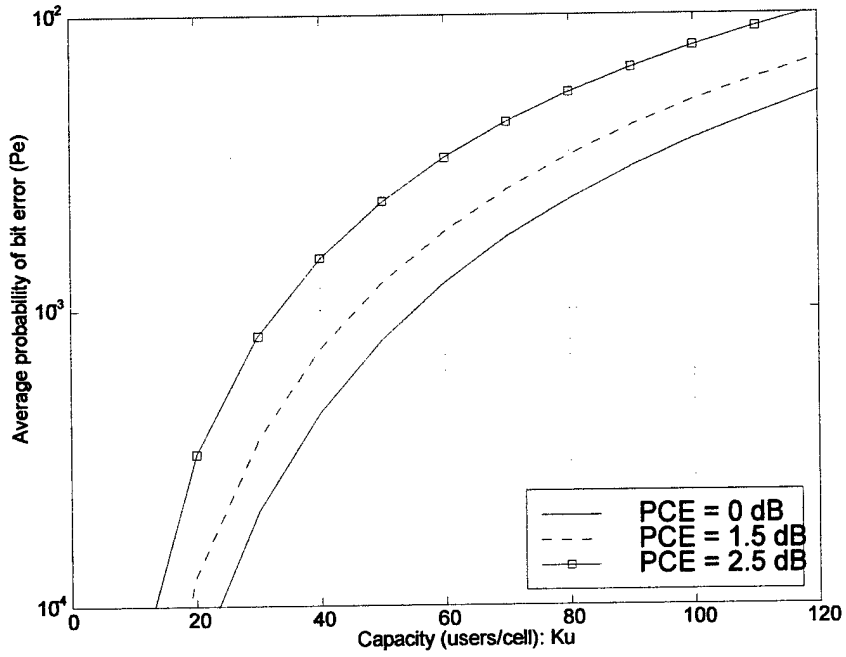

Figure 6.7: Average probability of bit error versus capacity. Four antenna elements, $M = 4$, various PCE's, and $p = 3/8$.

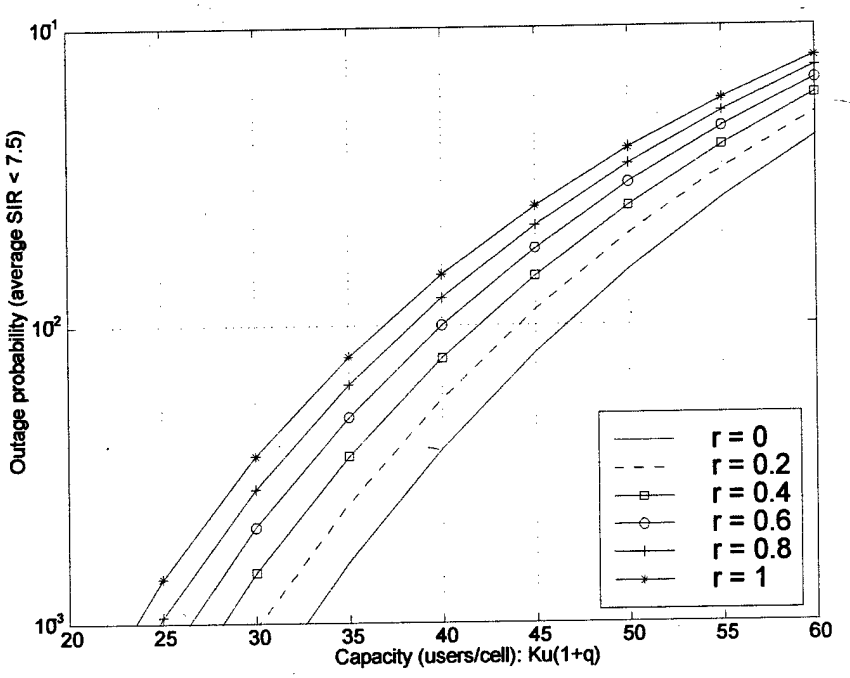

Figure 6.8: Outage probability versus capacity (users/cell), based on *average* SIR. Four antenna elements $M = 4$, four resolvable paths $L = 4$, PCE = 1.5 dB, different values of correlation coefficient r, and $p = 3/8$.

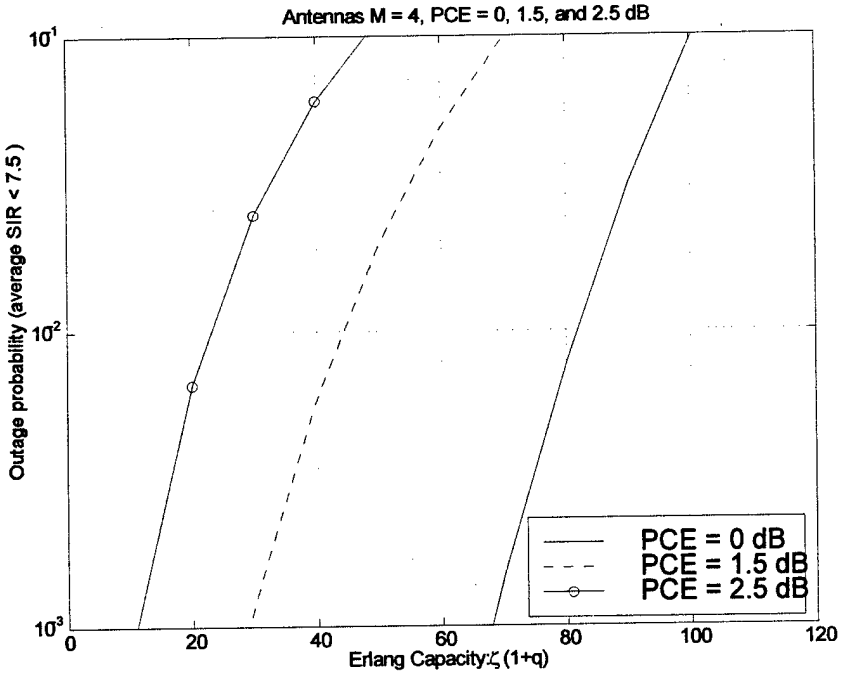

Figure 6.9: Outage probability versus Erlang capacity, based on *average* SIR. Four antenna elements $M = 4$, one resolvable path $L = 1$, $r = 0$, different PCE's, and $p = 3/8$.

Chapter 7

Reduced-Rank Array Processing Techniques

In this chapter, we study the application of the eigencanceler, a reduced rank method based on the eigendecomposition of the estimated covariance matrix, to the wireless communication problem in the presence of cochannel interference. The eigencanceler's performance is compared to that of a system utilizing sample matrix inversion (SMI). The application of SMI and the eigencanceler to a flat fading TDMA system is studied in the context of the IS-54/IS-136 standard.

7.1 BER Bound with Training Data

Based on the signal model in Chapter 2, the optimal combiner output is given by

$$y = \mathbf{w}^H \mathbf{u}$$

where the optimal weight vector is $\mathbf{w} = \mathbf{R}^{-1}\mathbf{c}_s$. Scaling of the weight vector has no effect on the output, hence the weight vector can also be expressed $\mathbf{w} = \mathbf{R}^{-1}\mathbf{r}$, where $\mathbf{r} = E[a[k]\,\mathbf{u}[k] \mid \mathbf{c}_s] = \sqrt{P_s}\mathbf{c}_s$ is the cross-correlation vector between the desired signal symbol and the received vector. The output SNR conditioned on the channel $\mathbf{c}_s$ is then given by

$$\mu = \|\mathbf{c}_s\|^2 \frac{P_s}{N_o} = \|\mathbf{c}_s\|^2 h, \tag{7.1}$$

where $\|\cdot\|^2$ denotes the Euclidean norm. Subsequent to the Gaussian assumption on the CCI, the conditional BER is given by $P(e \mid \mu) = Q\left(\sqrt{2\mu}\right)$, where Q is the Gaussian tail function.

Let $\lambda_i, i = 1, \ldots, N$ denote the eigenvalues of the noise covariance matrix $\mathbf{R}$ in descending order, $\lambda_1 \geq \lambda_2 \geq \ldots$ Assume that the L interference sources result in a noise covariance matrix with $r < N$ principal eigenvalues, such that $\lambda_r \gg \lambda_{r+1} = \ldots = \lambda_N = N_o$. It can be shown that the upper bound on the average BER is given by [19]

$$P_e < 0.5\,(1+h)^{-(N-r)}. \tag{7.2}$$

In practice, the true noise covariance matrix $\mathbf{R}$ as well as the cross-correlation vector $\mathbf{r}$, are not available and need to be estimated from the data. Assuming the availability of a training sequence of length K, the cross-correlation vector is estimated from the expression $\widehat{\mathbf{r}} = 1/K \sum_{k=1}^{K} a[k]\,\mathbf{u}[k]$. The estimated cross-correlation can then be used to estimate the interference vector $\widehat{\mathbf{x}}[k] = \mathbf{u}[k] - a[k]\widehat{\mathbf{r}}$. The estimated interference and noise covariance matrix is given by $\widehat{\mathbf{R}} = 1/K \sum_{k=1}^{K} \widehat{\mathbf{x}}[k]\widehat{\mathbf{x}}[k]^H$. We assume that $\mathbf{r} = \widehat{\mathbf{r}}$, and focus on the effect of estimating the covariance matrix. The goal is to investigate the effect of $\widehat{\mathbf{R}}$ on expression (7.2). In the following, it is assumed that the covariance matrix is estimated from a training set $\widehat{\mathbf{x}}(k)$, $k = 1, \ldots, K$. The training set is assumed to have the same statistics as the interference-plus-noise during normal operation, i.e., $\widehat{\mathbf{x}}(k)$ has a multivariate Gaussian distribution with zero-mean and covariance $\mathbf{R}$. We define the conditioned signal-to-noise and interference ratio (CSNR) ρ as the ratio of the SNIR when a specified weight vector $\mathbf{w}$ is used, to the optimal SNIR, $\mathbf{r}^H\mathbf{R}^{-1}\mathbf{r}$. The CSNR is then given by

$$\rho = \frac{\left|\mathbf{w}^H\mathbf{r}\right|^2}{\mathbf{w}^H\mathbf{R}\mathbf{w}} \frac{1}{\mathbf{r}^H\mathbf{R}^{-1}\mathbf{r}}. \tag{7.3}$$

The quantity ρ is a random variable that takes on values $0 \leq \rho \leq 1$, ($\rho = 1$ when $\mathbf{w} = \mathbf{R}^{-1}\mathbf{r}$) and with density $f_\rho(\rho)$. The BER conditioned on both the channel and CSNR is $P(e \mid \rho, \mu) = Q\left(\sqrt{2\rho\mu}\right)$. The performance penalty is made evident by the inequality $Q\left(\sqrt{2\rho\mu}\right) \geq Q\left(\sqrt{2\mu}\right)$. The mean BER can be found by averaging over both the CSNR and fading:

$$P_e = \int_0^\infty \int_0^1 P(e \mid \rho, \mu)\, f_\rho(\rho)\, f_\mu(\mu)\; d\mu d\rho, \tag{7.4}$$

where $f_\mu(\mu)$ is the density of μ [19]. We proceed to analyze the BER for two different methods of deriving the weight vector $\mathbf{w}$. The *sample matrix inversion* (SMI) weight vector is given by $\mathbf{w} = \widehat{\mathbf{R}}^{-1}\mathbf{r}$. The CSNR becomes

$$\rho = \frac{\left(\mathbf{r}^H\widehat{\mathbf{R}}^{-1}\mathbf{r}\right)^2}{\mathbf{r}^H\widehat{\mathbf{R}}^{-1}\mathbf{R}\widehat{\mathbf{R}}^{-1}\mathbf{r}} \frac{1}{\mathbf{r}^H\mathbf{R}^{-1}\mathbf{r}}. \tag{7.5}$$

The density of ρ for the SMI has been found in the classical paper [72], and is given by the beta function

$$f_\rho(\rho) = \frac{\Gamma(K+1)}{\Gamma(N-1)\,\Gamma(K+2-N)} (1-\rho)^{N-2}\, \rho^{K+1-N}. \tag{7.6}$$

We first evaluate $P(e \mid \mu) = \int_0^1 P(e \mid \rho, \mu)\, f_\rho(\rho)\, d\rho$. Using $Q\left(\sqrt{2\rho\mu}\right) < 0.5e^{-\rho\mu}$ and [73, relation 13.2.1], it can be shown that

$$P(e \mid \mu) < 0.5\,{}_1F_1(K+2-N, K+1, -\mu), \tag{7.7}$$

where ${}_1F_1$ is the confluent hypergeometric function. This expression is dependent on the number of samples K used to estimate the covariance matrix. Using (7.7) and the Kummer transformation ${}_1F_1(a, b, -\mu) = e_1^{-\mu}F_1(b-a, b, \mu)$ [73, relation 13.2.1], we obtain the

expression

$$P_e < 0.5\Gamma^{-1}(N-r)h^{-(N-r)} \int_0^\infty e^{-\mu(1+1/h)}\mu^{-(N-r-1)}{}_1F_1\left(N-1, K+1; \mu\right) d\mu, \tag{7.8}$$

which is recognized as a Laplace transform. Applying relation [74, p. 510], and after some algebra, this transform is evaluated as

$$P_e < 0.5\left(1+h\right)^{-(N-r)}\ {}_2F_1\left(N-1, N-r, K+1; h/\left(1+h\right)\right), \tag{7.9}$$

where ${}_2F_1$ is the Gauss hypergeometric function. This result is consistent with (7.2), since as the number of training samples

$$K \to \infty, \lim_{K\to\infty}\ {}_2F_1\left(N-1, N-r, K+1; h/\left(1+h\right)\right) = 1$$

[60, p.3], and (7.9) reverts to (7.2). The effect of finite K can be assessed by evaluating the function ${}_2F_1$. This function is available in software packages such as Mathematica, or it can be approximated by a series. Better insight into the effect of training is obtained by applying the asymptotic expansion of ${}_2F_1$, [75, p. 238]:

$${}_2F_1\left(a, b, c+m; z\right) = 1 + \frac{abz}{m} + o\left(m^{-2}\right), \tag{7.10}$$

where $m > 0$. For the problem at hand, we have

$${}_2F_1\left(N-1, N-r, K+1; h/\left(1+h\right)\right) = 1 + \frac{\left(N-1\right)\left(N-r\right)}{K}\frac{h}{1+h} + o\left(K^{-2}\right). \tag{7.11}$$

Substitution of (7.11) in (7.9) yields

$$P_e < 0.5\left(1+h\right)^{-(N-r)}\left(1 + \frac{\left(N-1\right)\left(N-r\right)}{K}\frac{h}{1+h} + o\left(K^{-2}\right)\right). \tag{7.12}$$

The significance of this relation is that for a given interference rank r, the BER increases *quadratically* with the number of degrees of freedom.

The SMI performance is compared with that of the eigencanceler. The eigencanceler is derived from the eigendecomposition of $\widehat{\mathbf{R}}$, and its weight vector when the interference rank is r, is given by $\mathbf{w} = \left(\mathbf{I} - \widehat{\mathbf{Q}}_1\widehat{\mathbf{Q}}_1^H\right)\mathbf{r}$ [76], where the columns of $\widehat{\mathbf{Q}}_1$ are the r eigenvectors associated with the principal eigenvalues of the sample covariance matrix $\widehat{\mathbf{R}}$. It can be shown that for large INR, the density function of the CSNR ρ for the eigencanceler is given by [77]:

$$f_\rho(\rho) = \Gamma^{-1}\left(r\right)K^r e^{-K(1-\rho)}\left(1-\rho\right)^{r-1}. \tag{7.13}$$

Using (7.13) in (6.25), we evaluate the conditional BER bound $P\left(e \mid \mu\right) < 0.5\int_0^1 e^{-\mu} f_\rho\left(\rho\right) d\rho$. We make the assumption that the values of the output SNR μ for which the density function

is non-vanishing are such that $\mu < K$. With this assumption, the previous integral can be evaluated as

$$P(e \mid \mu_0) < 0.5e^{-\mu}\left(1-\frac{\mu}{K}\right)^{-r}\left[1-\frac{\Gamma(r, K-\mu)}{\Gamma(r)}\right], \tag{7.14}$$

where $\Gamma(a,x) = \int_x^\infty e^{-t}t^{a-1}dt$. The series expansion of the terms in the parenthesis yields

$$P(e \mid \mu_0) < 0.5e^{-\mu}\left[1+\frac{\mu r}{K}+o\left(\frac{\mu}{K}\right)^2\right]\left[1-\frac{e^{-(K-\mu)}(K-\mu)^{r-1}}{\Gamma(r)}\left(1+o(K-\mu)^{-1}\right)\right]. \tag{7.15}$$

Keeping only the first order terms of K, and assuming $K \gg \mu$, the conditional BER is bound by

$$P(e \mid \mu) < 0.5e^{-\mu}\left(1+\frac{\mu r}{K}\right). \tag{7.16}$$

Substitution of (7.16) in (6.25) yields:

$$P_e < 0.5(1+h)^{-(N-r)}\left(1+\frac{r(N-r)}{K}\frac{h}{1+h}+o\left(K^{-2}\right)\right) \tag{7.17}$$

For large K, this expression can be approximated by the first two terms in the parenthesis. The eigencanceler's advantage over SMI is evident in the *linear* rather than *quadratic* increase in BER as a function of the degrees of freedom N.

7.2 Numerical Results

The theory developed above is illustrated through numerical results obtained from simulations. The simulation model consisted of two sources: a desired signal with specified SNR and an interference with INR = 2 dB. The modulation was BPSK, the number of antenna elements $N = 9$, and the number of training samples used for estimating the covariance matrix $K = 14$ (this conforms with the training specified by the IS-54/IS-136 TDMA standards). The fit between simulation data and theory is illustrated in Figure 62. The simulation results represent the error count of 280,000 Monte Carlo runs. The channel was assumed fixed over the processing interval, but was varied randomly from run to run. Theoretical curves were generated by evaluating the integral in (6.25) numerically, using the SMI and eigencanceler probability density expressions in (7.6) and (7.13), respectively. A good fit is observed between theory and simulations.

The error bounds and the exact BER expressions are compared in Figure 62 as a function of the SNR for the case of $K = 14$ training symbols. The approximations are based on (7.12) and (7.17), respectively. An error of about 1 dB is observed between the bound and the exact values. The bound error has three sources: (1) error due to the approximation of the Gaussian tail function with the quantity $0.5e^{-\mu}$, (2) error due to the assumption that INR is large, (3) error due to the assumption that K is large. The Gaussian tail approximation is the main source of the bound error. The INR provides negligible error. This is explained by the well known fact that the output of an adaptive array with sufficient degrees of freedom and optimum combining is not very sensitive to the interference power.

7.3 Application to IS-54/IS-136

The IS-54/IS-136 TDMA system uses $\pi/4$-shifted DQPSK modulation. The probability of symbol error for $\pi/4$ -DQPSK is given by [78]:

$$P_e(\mu) = \frac{1}{4\pi\sqrt{2}} \int_0^{2\pi} \frac{1}{1 - \frac{\cos t}{\sqrt{2}}} \exp\left[-\mu\left(1 - \frac{\cos t}{\sqrt{2}}\right)\right] dt. \tag{7.18}$$

A typical IS-54 TDMA frame contains $K = 14$ synchronization symbols that can also be used for array training. Performance of a TDMA system with an antenna array controlled by the SMI or eigencanceler methods was evaluated by simulation. The signal environment was modeled by three cell layers. With all channels fully occupied, interference was provided by 6 CCI sources from the first layer, 12 CCI sources from the second layer, and 18 CCI sources from the third layer, while ignoring interferences from other outlying layers. CCI sources were assumed to be the base stations of the surrounding cells. The normalized eigenvalue distribution of a sample interference and noise covariance matrix for an $N = 9$ element antenna is shown in Figure 63. Note that most of the interference power is concentrated in the 6 largest eigenvalues, suggesting the use of a reduced-rank method such as the eigencanceler. Figure 63 shows the average BER versus the carrier-to-interference ratio (CIR) for an adaptive array with E_b/N_o= 10 dB. The capacity of a TDMA system is expressed in terms of its reuse factor. Current 2G standards stipulate a frequency reuse factor of 7. The curves shown in the figure are averages of 1000 runs. Each run consisted of estimation of the array covariance matrix $\widehat{\mathbf{R}}$ using $K = 14$ training samples, and a randomly chosen channel vector $\mathbf{c}_s$. Reuse factors are marked by arrows. For BER $= 10^{-3}$, SMI can be applied with reuse factor 3, while the eigencanceler provides higher capacity corresponding to a reuse factor of 1.

7.4 Discussion

This chapter considered reduced-rank antenna arrays for wireless communications. The content focused on the eigencanceler, but other reduced rank methods can be applied. Simple analytical expressions were obtained for the BER bound for the case of BPSK modulation and the presence of colored Gaussian CCI. The performance of a TDMA system as specified by the IS-54/IS-136 standards was studied by simulation. It was shown that reduced-rank processing at the base station can increase the capacity of TDMA systems by reducing the frequency reuse factor from 7 to 1.

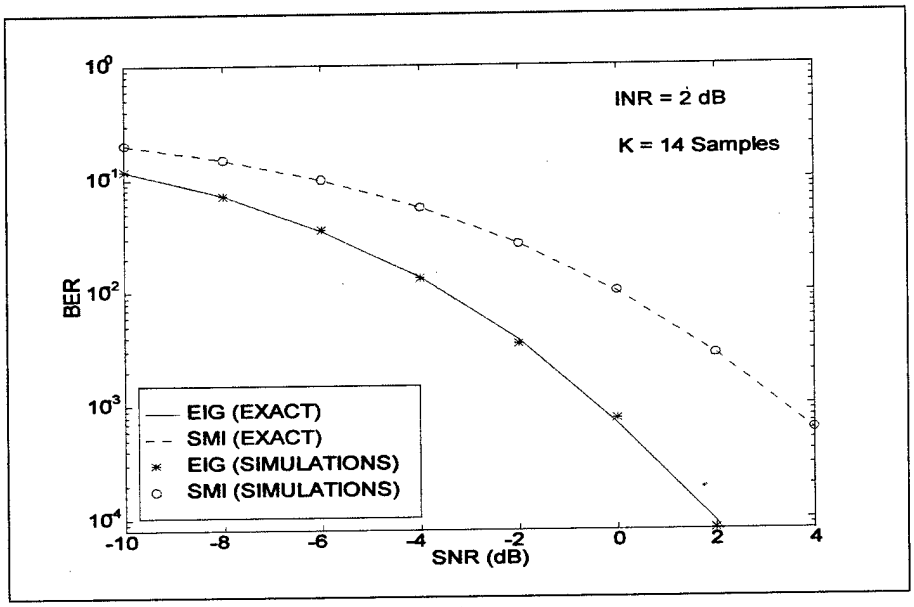

Figure 7.1: Comparison of theoretical expressions and simulation results.

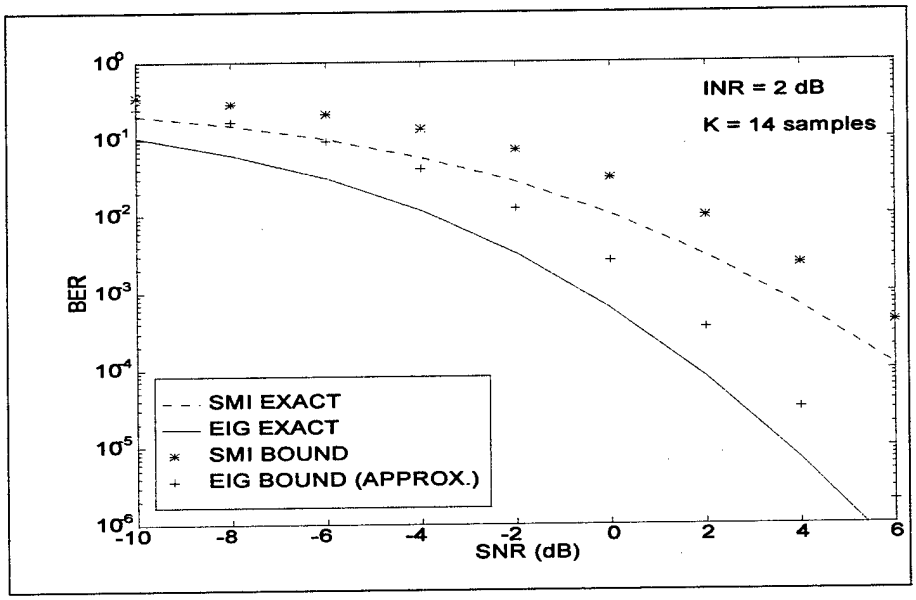

Figure 7.2: Bound and exact BER for SMI and eigencanceler with $N = 9$ elements and $K = 14$ training samples.

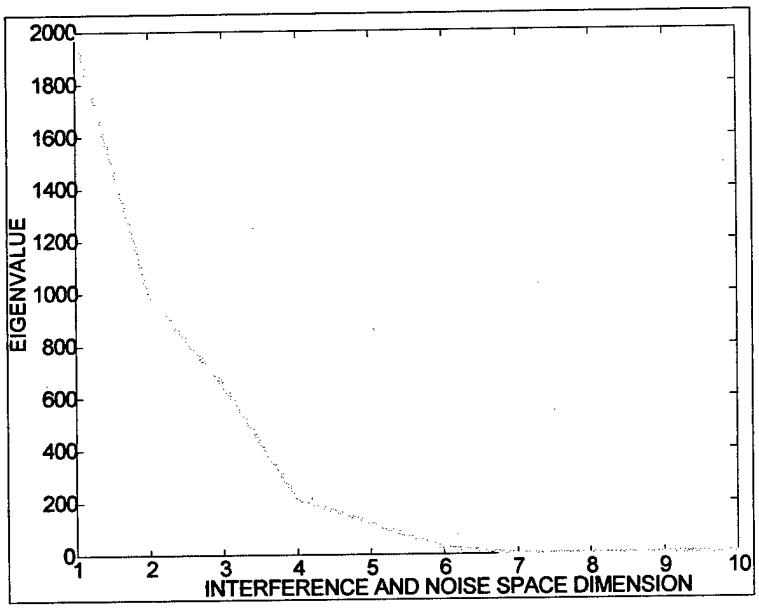

Figure 7.3: Eigenvalues of interference plus noise covariance matrix.

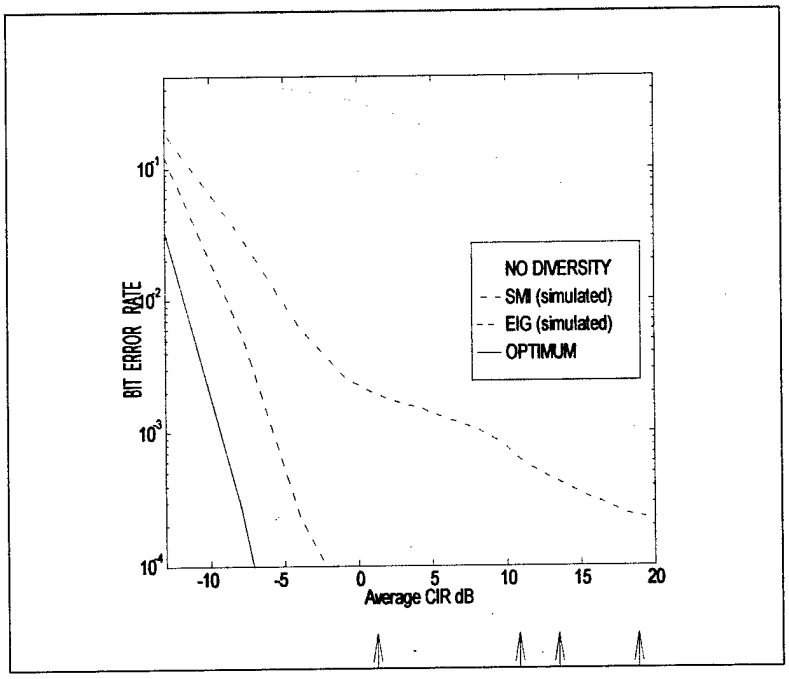

Figure 7.4: Average BER vs. CIR. Arrows indicate the corresponding reuse factor.

Appendix A

Appendix

This section contains the derivation of (4.61). The average BER is given by

$$\begin{aligned} P_e &= \frac{1}{2}\int_0^\infty \operatorname{erfc}(\sqrt{\mu}) f_\mu(\mu) d\mu \\ &= \frac{1}{2}\frac{\Gamma(L+1)}{\Gamma(N)\Gamma(L+1-N)}\left(\frac{P_s}{P}\right)^{L+1-N}\int_0^\infty \operatorname{erfc}(\sqrt{\mu})\frac{\mu^{N-1}}{(\frac{P_s}{P}+\mu)^{L+1}}d\mu. \end{aligned} \tag{A-1}$$

Using the identity [55]

$$\operatorname{erfc}(\sqrt{\mu}) = \frac{\mu^{-\frac{1}{4}}}{\sqrt{\pi}} e^{-\frac{\mu}{2}} W_{-\frac{1}{4},\frac{1}{4}}(\mu), \tag{A-2}$$

in (A-1), we get

$$P_e = \frac{1}{2\sqrt{\pi}}\frac{\Gamma(L+1)}{\Gamma(N)\Gamma(L+1-N)}\left(\frac{P_s}{P}\right)^{L+1-N}\int_0^\infty \frac{\mu^{N-\frac{5}{4}}}{(\frac{P_s}{P}+\mu)^{L+1}} e^{-\frac{\mu}{2}} W_{-\frac{1}{4},\frac{1}{4}}(\mu) d\mu, \tag{A-3}$$

where $W_{p,q}(\cdot)$ is the Whittaker function of the second kind and is defined as

$$W_{p,q}(x) = \frac{x^p e^{-\frac{x}{2}}}{\Gamma(q-p+\frac{1}{2})}\int_0^\infty e^{-t} t^{(q-p-\frac{1}{2})}(1+\frac{t}{x})^{(q+p-\frac{1}{2})} dt, \quad q-p+\frac{1}{2} > 0. \tag{A-4}$$

Equation (A-3) can be evaluated in a closed form and is [79]:

$$P_e = \frac{1}{2\sqrt{\pi}\Gamma(N)\Gamma(L+1-N)}\left(\frac{P_s}{P}\right)^{\frac{-1}{4}} G_{2,3}^{3,1}\left(\frac{P_s}{P}\,\middle|\, \begin{matrix} -N+\frac{5}{4}, \frac{5}{4} \\ L-N+\frac{5}{4}, \frac{3}{4}, \frac{1}{4} \end{matrix}\right), \tag{A-5}$$

where $G_{p,q}^{m,n}(\cdot)$ is the Meijer's G-function and is defined as [79]

$$\mathrm{G}_{p,q}^{m,n}\left(x\,\middle|\, \begin{matrix} a_1, \ldots, a_p \\ b_1, \ldots, b_q \end{matrix}\right) = \frac{1}{2\pi i}\int_C \frac{\prod_{j=1}^m \Gamma(b_j - s)\prod_{j=1}^n \Gamma(1-a_j+s)}{\prod_{j=m+1}^q \Gamma(1-b_j+s)\prod_{j=n+1}^p \Gamma(a_j-s)} x^s ds, \tag{A-6}$$

where C is a curve separating the poles of $\prod_{j=1}^{m}\Gamma(b_j-s)$ from those of $\prod_{j=1}^{n}\Gamma(1-a_j+s)$, $1\le q$, $0\le n\le p\le q$, $0\le m\le q$; $x\neq 0$ and $|\,x\,|<1$ if $q=p$; $x\neq 0$ if $q>p$. See [80] for more definitions and evaluation of the G-function. Using the identity [79]

$$G_{p,q}^{q,1}\left(x\,\middle|\,\begin{matrix}a_1,\dots a_p\\ ,\dots b_q\end{matrix}\right)= x^{a_1-1}E\left(1-a_1+b_1,\dots,1-a_1+b_q:1-a_1+a_2,\dots,1-a_1+a_p:x\right), \tag{A-7}$$

in (A-5), we get

$$P_e=\frac{1}{2\sqrt{\pi}\Gamma(N)\Gamma(L+1-N)}\left(\frac{P_s}{P}\right)^{-N}E\left(L+1,N+\frac{1}{2},N:N+1:\frac{P_s}{P}\right), \tag{A-8}$$

where $E(\cdot)$ is the MacRobert's E-function and is defined as [79]

$$E\left(a_1,\dots,a_p:b_1,\dots,b_q:x\right)= \tag{A-9}$$

$$\sum_{r=1}^{p}\frac{\hat{\prod}_{s=1}^{p}\Gamma(a_s-a_r)}{\prod_{t=1}^{q}\Gamma(b_t-a_r)}\Gamma(a_r)x^{a_r}$$

$${}_{q+1}F_{p-1}\left(a_r,a_r-b_1+1,\dots,a_r-b_q+1;a_r-a_1+1,\dots,*,\dots,a_r-a_p+1;(-1)^{p-q}x\right), \tag{A-10}$$

where ${}_pF_q(\cdot)$ is the generalized hypergeometric series and is as defined in (4.62). The $\hat{}$ in $\hat{\prod}$ denotes the omission of the term when $s=r$. Also, the $*$ in ${}_pF_q(\cdot)$ indicates omission of the term (a_r-a_r+1). Equation (A-9) is valid for $p\ge q+1$. Using identity of (A-9) in (A-8) and ${}_2F_2\left(N,0;N-L,\frac{1}{2};\frac{P_s}{P}\right)=1$, we get

$$\begin{aligned}P_e &= \frac{1}{2\sqrt{\pi}\Gamma(N)\Gamma(L+1-N)}\left(\frac{P_s}{P}\right)^{-N}\left[\left(\frac{P_s}{P}\right)^{L+1}\frac{\Gamma(N-L-\frac{1}{2})\Gamma(N-L-1)\Gamma(L+1)}{\Gamma(N-L)}\right. \qquad \text{(A-11)}\\ &\quad {}_2F_2\left(L+1,L+1-N;L-N+\frac{3}{2},L-N+2;\frac{P_s}{P}\right)+\left(\frac{P_s}{P}\right)^{N+\frac{1}{2}}\frac{\Gamma(L-N+\frac{1}{2})}{\Gamma(\frac{1}{2})}\\ &\quad \Gamma(-\frac{1}{2})\Gamma(N+\frac{1}{2}){}_2F_2\left(N+\frac{1}{2},\frac{1}{2};N-L+\frac{1}{2},\frac{3}{2};\frac{P_s}{P}\right)+\left(\frac{P_s}{P}\right)^{N}\frac{\Gamma(L+1-N)\Gamma(\frac{1}{2})}{\Gamma(1)}\\ &\quad \left.\Gamma(N){}_2F_2\left(N,0;N-L,\frac{1}{2};\frac{P_s}{P}\right)\right]\\ &= \frac{1}{2\sqrt{\pi}\Gamma(N)\Gamma(L+1-N)}\left[\left(\frac{P_s}{P}\right)^{L+1-N}\frac{\Gamma(N-L-\frac{1}{2})\Gamma(L+1)}{(N-L-1)}\right.\\ &\quad {}_2F_2\left(L+1,L+1-N;L-N+\frac{3}{2},L-N+2;\frac{P_s}{P}\right)+\left(\frac{P_s}{P}\right)^{\frac{1}{2}}\frac{\Gamma(L-N+\frac{1}{2})}{\Gamma(\frac{1}{2})}\\ &\quad \left.\Gamma(-\frac{1}{2})\Gamma(N+\frac{1}{2}){}_2F_2\left(N+\frac{1}{2},\frac{1}{2};N-L+\frac{1}{2},\frac{3}{2};\frac{P_s}{P}\right)+\frac{\Gamma(L+1-N)\Gamma(\frac{1}{2})\Gamma(N)}{\Gamma(1)}\right]. \qquad \text{(A-12)}\end{aligned}$$

Reference

Bibliography

[1] A. Shah and A.M. Haimovich, "Performance Analysis of Optimum Combining in Wireless Communications with Rayleigh Fading and Cochannel Interference," *IEEE Transactions on Communication*, vol. 46, pp. 473–479, April 1998.

[2] A. Shah and A. Haimovich , "A performance comparison of optimum combining and maximal ratio combining for digital cellular radio communications systems with cochannel interference," *IEEE Transactions on Vehicular Technology, to be published.*

[3] A. Shah and A. Haimovich and M.K. Simon and M.S. Alouini , "Exact bit error probability for optimum combining with a Rayleigh fading co-channel interferer," *IEEE Transactions on Communications, to be published.*

[4] W. Ye and A. Haimovich, "Performance of cellular CDMA systems with space diversity, fading, and imperfect power control," *Proceeding of the 48th IEEE Vehicular Technology Conference, Otawa, Canada*, pp. 1868–1872, May 18-21 1998.

[5] W. Ye and A. Haimovich, "Probability of bit error in power controlled cellular CDMA systems with space diversity," *presented at the Thirty Second Annual Conference on Information Sciences and Systems, Princeton, NJ*, March 19-22 1998.

[6] W. Ye, A. Haimovich, "Outage probability of cellular CDMA systems with space diversity, Rayleigh fading, and power control error," *IEEE Communications Letters*, vol. 2, pp. 220–222, August 1998.

[7] W. Ye and A. Haimovich , "Performance of cellular CDMA with cell site antenna arrays, Rayleigh fading and power control error," *IEEE Transactions on Communications, to be published.*

[8] A. Haimovich and A. Shah, "STAP in wireless communications: Performance analysis," *ASAP'97 Fifth Annual Adaptive Sensor Array Processing Workshop, M.I.T. Lincoln Labs,Lexington, MA.*, pp. 685–714, March 12-14 1997.

[9] A. Shah and A. Haimovich, "Applications of space-time processing in wireless communications," *Proceedings of MILCOM'97, Monterey, CA.*, November 2-5 1997.

[10] A. Haimovich and A. Shah and X. Wu , "Reduced-rank processing for wireless communications with applications to IS-54/IS-136," *IEEE Transactions on Communications, to be published.*

[11] W. C. Jakes, Jr., *Microwave Mobile Communication.* New York, USA: John Wiley & Sons, Inc., 1974.

[12] J. H. Winters, "Optimum Combining in Digital Mobile Radio with Cochannel Interference," *IEEE Transactions on Vehicular Technology*, vol. 33, pp. 144–155, August 1984.

[13] P. Y. Kam, "Bit Error Probabilities of MDPSK Over the Nonselective Rayleigh Fading Channel with Diversity Reception," *IEEE Transactions on Communications*, vol. 39, pp. 220–224, February 1991.

[14] N. C. Beaulieu and A. A. Abu-Dayya, "Analysis of Equal Gain Diversity on Nakagami Fading Channels," *IEEE Transactions on Communications*, vol. 39, pp. 225–233, February 1991.

[15] A. A. Abu-Dayya and N. C. Beaulieu, "Outage Probabilities of Diversity Cellular Systems with Cochannel Interference in Nakagami Fading," *IEEE Transactions on Vehicular Technology*, vol. 41, pp. 343–355, November 1992.

[16] A. A. Abu-Dayya and N. C. Beaulieu, "Microdiversity on Rician Fading Channels," *IEEE Transactions on Communications*, vol. 42, pp. 2258–2267, June 1994.

[17] Q. T. Zhang, "Probabilty of Error for Equal-Gain Combiners over Rayleigh Channels: Some Closed-Form Solutions," *IEEE Transactions on Communication*, vol. 45, pp. 270–273, March 1997.

[18] V. Bogachev and I. Kiselev, "Optimum Combining of Signals in Space-Diversity Reception," *Telecommunications and Radio Engineering*, vol. 34/35, pp. 83–85, October 1980.

[19] A. M. Haimovich and A. Shah, "The Performance of Space-Time Processing for Suppressing Narrowband Interference in CDMA communications," *Wireless Personal Communications*, vol. 7:2-3, pp. 233–255, June 1998.

[20] N. C. Beaulieu and A. A. Abu-Dayya, "Bandwidth Efficient QPSK in Cochannel Interference and Fading," *IEEE Transactions on Communication*, vol. 43, pp. 2464–2474, September 1995.

[21] H. Gao, "The Design and Analysis of Some Computationally Intensive Communication Systems," *Doctoral Dissertation, Victoria University of Wellington*, April 1996.

[22] V. Bogachev and I. Kiselevs, "Optimum combining of signals in space-diversity reception," *Tele. Radio Eng.*, vol. 34/35, pp. 83–85, October 1980.

[23] J. Winters, "Optimum combining in digital mobile radio with co-channel interference," *IEEE Trans. on Vehic. Tech*, vol. VT-33, pp. 144–155, August 1984.

[24] A. A. Abu-Dayya and N. C. Beaulieu, "Outage probability in the presence of correlated lognormal interferers," *IEEE Trans. Vehicular Technology*, vol. 43, pp. 164–173, Feb. 1994.

[25] A. M. Viterbi and A. J. Viterbi, "Erlang capacity of a power controlled CDMA system," *IEEE J. Select. Areas Commun.*, vol. 11, pp. 892–900, Aug. 1993.

[26] K. S. Gilhousen, I. M. Jacobs, R. Padovani, A. J. Viterbi, L. A. Weaver, and C. E. Wheatley, "On the capacity of a cellular CDMA system," *IEEE Trans. Vehicular Technology*, vol. 40, pp. 303–312, May 1991.

[27] Y. S. Yeh and S. C. Schwartz, "Outage probability in mobile telephony due to multiple log-normal interferers," *IEEE Trans. communications.*, vol. 32, pp. 380–388, Apr. 1984.

[28] A. J. Viterbi, A. M. Viterbi, and E. Zehavi, "Performance of power-controlled wideband terrestrial digital communication," *IEEE Trans. communications.*, vol. 41, pp. 559–569, Apr. 1993.

[29] M. Soleimanipour and G. H. Freeman, "A realistic approach to the capacity of cellular CDMA systems," in *IEEE 46th Vehicular Technology Conference Proceedings*, (Atlanta, GA), pp. 1125–9, Apr.28 - May 1 1996.

[30] M. Zorzi and S. Pupolin, "Outage probability in multiple access interference radio networks in the presence of fading," *IEEE Trans. Vehicular Technology*, vol. 43, pp. 604–610, Aug. 1994.

[31] M. Zorzi, "On the analytical computation of the interference statistics with applications to the performance evaluation of mobile radio systems," *IEEE Trans. communications.*, vol. 45, pp. 103–109, Jan. 1997.

[32] A. F. Naguib, "Power control in wireless CDMA: performance with cell site antenna arrays," in *Proceedings of IEEE 1995 Global Telecommunications Conference*, (Singapore), pp. 225–229, Nov. 1995.

[33] B. R. Vojcic, R. L. Pickholtz, and L. B. Milstein, "Performance of DS-CDMA with imperfect power control operating over a low earth orbiting satellite link," *IEEE Journal on Selected Areas in Communications*, vol. 12, pp. 560–567, May 1994.

[34] F. Vatalaro, G. E. Corazza, F. Ceccarelli, and G. D. Maio, "A realistic approach to the capacity of cellular CDMA systems," in *IEEE 46th Vehicular Technology Conference Proceedings*, (Atlanta, GA), pp. 1125–9, Apr.28- May 1 1996.

[35] N. Kong and L. B. Milstein, "Approximations to and chernoff bound on the error probabilities of multicell CDMA over a multipath fading channel with power control error," in *Proceedings of the 1996 Conference on Information Science and Systems*, (Princeton, NJ), pp. 1131–1135, Mar. 1996.

[36] I. P. Kirsteins and D. W. Tufts, "Adaptive detection using low rank approximation to data matrix," *IEEE Transactions on Aerospace and Electronic Systems*, vol. 30, pp. 55–67, Jan. 1994.

[37] A. Haimovich, "The eigencanceler: Adaptive radar by eigenanalysis methods," *IEEE Transactions on Aerospace and Electronic Systems*, vol. 32, pp. 532–542, April 1996.

[38] J. G. Proakis, *Digital Communications.* New York, USA: McGraw-Hill, 3rd ed., 1995.

[39] J.B. Seaborn, *Hypergeometric Functions and Their Applications.* New York, USA: Springer-Verlag, 1991.

[40] A. T. James, "Distributions of Matrix Variates and Latent Roots Derived from Normal Samples," *Annals of Mathematical Statistics*, vol. 35, pp. 475–501, 1964.

[41] N. R. Goodman, "Statistical Analysis Based on a Certain Multivariate Complex Gaussian Distribution (An Introduction)," *Annals of Mathematical Statistics*, vol. 34, pp. 152–177, 1963.

[42] A. A. Abu-Dayya and N. C. Beaulieu, "Outage Probabilities of Cellular Mobile Radio Systems with Multiple Nakagami Interferers," *IEEE Transactions on Vehicular Technology*, vol. 40, pp. 757–768, November 1991.

[43] A. P. Prudnikov, Y. A. Brychkov and O. I. Marichev, *Integrals and Series*, vol. 4. Philadelphia, USA: Gordon and Breach Science Publishers, 1992.

[44] M. Abramowitz and I. A. Stegun, *Handbook of Mathematical Functions with Formulas, Graphs, and Mathematical Tables.* Washington D.C., USA: National Bureau of Standards, 1970.

[45] H. Cramer, *Random Variables and Probability Distributions.* New York, USA: Cambridge University Press, 1970.

[46] A. Shah, "Adaptive Space-Time Processing for Digital Mobile Radio Communication Systems," *Doctoral Dissertation, Electrical and Computer Engineering Department, New Jersey Institute of Technology*, May 1997.

[47] R. A. Monzingo and T. W. Miller, *Introduction to Adaptive Arrays.* New York, USA: John Wiley & Sons, Inc., 1980.

[48] N. C. Giri, *Multivariate Statistical Inference.* New York, USA: Academic Press, Inc., 1977.

[49] C. G. Khatri, "On Certain Distribution Problems Based on Positive Definite Quadratic Functions in Normal Vectors," *Annals of Mathematical Statistics*, vol. 37, pp. 468–479, 1968.

[50] R. J. Muirhead, *Aspects of Multivariate Statistical Theory.* New York, USA: John Wiley & Sons, Inc., 1982.

[51] M. S. Srivastava and C. G. Khatri, *An Introduction to Multivariate Statistics.* New York, USA: Elsevier North Holland, Inc., 1979.

[52] A. M. Kshirsagar, *Multivariate Analysis.* New York, USA: Marcel Dekker, Inc., 1972.

[53] Q. T. Zhang, "Outage Probability in Cellular Mobile Radio Due to Nakagami Signal and Interferers with Arbitrary Parameters," *IEEE Transactions on Vehicular Technology*, vol. 45, pp. 364–372, May 1996.

[54] I. S. Gradshteyn and I. M. Ryzhik, *Table of Integrals, Series and Products.* New York, USA: Academic Press, Inc., 1980.

[55] L. C. Andrews, *Special Functions for Engineers and Applied Mathematicians.* New York, USA: Macmillan Publishing Company, 1985.

[56] M. Simon and M. Alouini, "A unified approach to the performance analysis of digital communications over generalized fading channels," *Proceedings of the IEEE*, vol. 86 No.9, pp. 1860–1877, September 1998.

[57] J. DiFranco and W. Rubin, *Radar Detection.* NJ,USA: Prentice-Hall, Englewood Cliffs, 1968.

[58] L. Andrews, *Special Functions for Engineers and Applied Mathematicians.* New York: Macmillam Publishing Company.

[59] H. Exton, *Handbook of Hypergeometric Integrals.* Chichester, UK: Ellis Horwood Limited, 1978.

[60] W. Bailey, *Generalized Hypergeometric Series.* New-York: Stechert-Hafner Service Agency, 1964.

[61] I. Gradshteyn and I.M.Ryzhik, *Table of Integrals, Series, and Products.* San Diego,CA: Academic Press, fifth ed, 1994.

[62] S. C. Schwartz and Y. S. Yeh, "On the distribution function and moments of power sums with log-normal components," *The Bell System Technical Journal*, vol. 61, pp. 1441–1462, Sept. 1982.

[63] L. B. Milstein, T. S. Rappaport, and R. Barghouti, "Performance evaluation for cellular CDMA," *IEEE J. Select. Areas Commun.*, vol. 10, pp. 680–689, May 1992.

[64] N. Kong and L. B. Milstein, "Performance of multicell CDMA with power control error," in *Proceedings of IEEE 1995 Military Communications Conference*, (San Diego, CA), pp. 513–517, Nov. 1995.

[65] A. Leon-Garcia, *Probability and Random Processes for Electrical Engineering.* Reading, MA: Addison-Wesley Publishing Company, 1994.

[66] J. M. Holtzman, "A simple, accurate method to calculate spread-spectrum multiple-access error probabilities," *IEEE Trans. communications.*, vol. 40, pp. 461–464, Mar. 1992.

[67] A. J. Viterbi, A. M. Viterbi, and E. Zehavi, "Other-cell interference in cellular power-controlled CDMA," *IEEE Trans. Communications.*, vol. 42, pp. 1501–1504, Feb./Mar./Apr. 1994.

[68] A. J. Viterbi, *CDMA Principles of Spread Spectrum Communication.* Reading, MA: Addison-Wesley Publishing Company, 1995.

[69] A. Safak, "Statistical analysis of the power sum of multiple correlated log-normal components," *IEEE Trans. Vehicular Technology*, vol. 42, pp. 58–61, Feb. 1993.

[70] X. C. Bernstein and A. M. Haimovich, "Space-time optimum combining for CDMA communications," *Wireless Personal Communications*, vol. 3, pp. 73–89, 1996.

[71] S. A. Abbas and A. U. H. Sheikh, "Outage analysis due to multipath mobile radio reception with poisson multipath arrival," *Wireless Personal Communications*, vol. 5, pp. 173–193, Sept. 1997.

[72] I. S. Reed et. al., "Rapid convergence rates in adaptive arrays," *IEEE Transactions on Aerospace and Electronic Systems*, vol. 10, pp. 853–863, Nov. 1974.

[73] M. Abramowitz and I. A. Stegun, *Handbook of Mathematical Functions.* Washibgton, DC: National Bureau of Standards, 1972. Tenth printing.

[74] A. P. Prudnikov, Y. A. Brychkov, and O. I. Marichev, *Integrals and Series.* Philadelphia, PA: Gordon and Breach Science, 1992.

[75] Y. Luke, *The Special Functions and Their Approximations, Vol. 1.* New York: Academic Press, 1969.

[76] X. Wu and A. Haimovich, "Adaptive arrays for increased performance in mobile communications," in *Proceedings of the The Sixth Internationl Symposium on Personal, Indoor and Mobile Radio Communications (PIMRC'95)*, (Toronto, Canada), pp. 653–657, Sept. 1995.

[77] A. Haimovich, "Asymptotic distribution of the conditioned signal-to-noise ratio in an eigenanalysis-based adaptive array," *IEEE Transactions on Aerospace and Electronic Systems*, pp. 988–996, July 1997.

[78] F. Adachi, "Postdetection optimal diversity combiner for DPSK differential detection," *IEEE Transactions on Vehicular Technology*, vol. 42, pp. 326–337, Aug. 1993.

[79] A. Erdelyi et al., *Tables of Integral Transforms: Volume II.* New York, USA: McGraw-Hill, 1954.

[80] A. M. Mathai and R. K. Saxena, *Generalized Hypergeometric Functions with Applications in Statistics and Physical Sciences.* New York, USA: Springer-Verlag, Inc., 1973.